© 2015. Published by The Company of Biologists Ltd | Development (2015) 142, 2764-2774 doi:10.1242/dev.121962

RESEARCH ARTICLE

STEM CELLS AND REGENERATION

The thyroid hormone nuclear receptor TRα1 controls the Notch signaling pathway and cell fate in murine intestine

Maria Sirakov[1,*], Amina Boussouar[1,‡,§], Elsa Kress[1,‡,§], Carla Frau[1,‡], Imtiaz Nisar Lone[2], Julien Nadjar[1,‡], Dimitar Angelov[2] and Michelina Plateroti[1,‡,¶]

ABSTRACT

Thyroid hormones control various aspects of gut development and homeostasis. The best-known example is in gastrointestinal tract remodeling during amphibian metamorphosis. It is well documented that these hormones act via the TR nuclear receptors, which are hormone-modulated transcription factors. Several studies have shown that thyroid hormones regulate the expression of several genes in the Notch signaling pathway, indicating a possible means by which they participate in the control of gut physiology. However, the mechanisms and biological significance of this control have remained unexplored. Using multiple *in vivo* and *in vitro* approaches, we show that thyroid hormones positively regulate Notch activity through the TRα1 receptor. From a molecular point of view, TRα1 indirectly controls Notch1, Dll1, Dll4 and Hes1 expression but acts as a direct transcriptional regulator of the *Jag1* gene by binding to a responsive element in the *Jag1* promoter. Our findings show that the TRα1 nuclear receptor plays a key role in intestinal crypt progenitor/stem cell biology by controlling the Notch pathway and hence the balance between cell proliferation and cell differentiation.

KEY WORDS: Intestinal epithelium, Notch pathway, Thyroid hormones, Thyroid hormone nuclear receptor, *Thra*, Mouse

INTRODUCTION

The intestinal epithelium is a very dynamic tissue that is continuously renewed by stem cells and committed progenitors located in the crypts of Liberkühn (reviewed by Stappenbeck et al., 1998; Barker et al., 2010). Its development and homeostasis involve several signaling pathways, including Wnt, Hedgehog, Notch, BMP and thyroid hormones (THs) (reviewed by Sirakov and Plateroti, 2011; van der Flier and Clevers, 2009). By cross-regulating each other, these pathways maintain the balance in physiological conditions among key biological processes such as proliferation, differentiation and apoptosis. Importantly, their dysregulation is correlated with the induction and/or progression of pathologies such as colorectal cancer (Fre et al., 2009; Sirakov et al., 2012; Kress et al., 2010; reviewed by Radtke et al., 2006).

TH signaling is a key regulator of gastrointestinal development and homeostasis in both amphibians and mammals, where it regulates postnatal development (reviewed by Sirakov and Plateroti, 2011; Shi et al., 2011). THs act via the thyroid hormone nuclear receptors (TRs), which belong to the nuclear hormone receptor transcription factor superfamily (reviewed by Robinson-Rechavi et al., 2003) and are modulated in their activity by the hormone triiodothyronine (T3) (reviewed by Chin and Yen, 1996; Oetting and Yen, 2007). The TRs are encoded by the *Thra* and *Thrb* loci (Robinson-Rechavi et al., 2003), which produce several protein isoforms through the use of different promoters and alternative splicing (Chin and Yen, 1996; Oetting and Yen, 2007). In the case of the *Thra* gene, the TRα1 isoform is the only T3 nuclear receptor encoded by the locus (Oetting and Yen, 2007). TRs regulate the transcription of target genes by binding to specific DNA sequences termed thyroid hormone response elements (TREs) in a T3-independent manner; after T3 binding, co-repressors are released and co-activators recruited, promoting target gene transcription (Oetting and Yen, 2007). Studies on *Thra* and/or *Thrb* knockout animals showed that intestinal TH signaling is essentially mediated by TRα1 to control crypt cell proliferation (Plateroti et al., 1999, 2006). Notably, THs also affect the expression of several genes in the intestinal crypts (Kress et al., 2009) that have been described in the stem cell signature defined by the Lgr5 marker (Muñoz et al., 2012).

Our previous studies showed a complex functional interaction between TH-TRα1 and Wnt (Sirakov et al., 2012; Kress et al., 2010; Plateroti et al., 2006); however, we also collected evidence that THs control the expression of several genes of the Notch pathway (Kress et al., 2009). Importantly, together with the canonical Wnt pathway, Notch is currently receiving great attention because of its involvement in both intestinal development and cancer (VanDussen et al., 2012; Peignon et al., 2011; reviewed by Horvay and Abud, 2013). The Notch pathway acts through cell-cell interaction between a membrane-bound ligand belonging to the Jagged and Serrate protein family and a Notch membrane-bound receptor. After their interaction, the intracellular portion of the Notch receptor undergoes two consecutive proteolytic cleavage events, and the resulting active Notch intracellular domain (NICD) translocates into the nucleus and complexes with RBP-J or CSL transcription factors to regulate the expression of Notch target genes (Artavanis-Tsakonas et al., 1995). In the murine intestine, Notch signaling controls cell fate determination (reviewed by Fre et al., 2011a; Noah and Shroyer, 2013; Sancho et al., 2015). Specifically, Notch inhibition reduces crypt cell proliferation and induces secretory cell hyperplasia (van Es et al., 2005; Riccio et al., 2008; Pellegrinet et al., 2011); conversely, its constitutive activation expands the proliferative zone and represses secretory cell differentiation in developing and adult intestine (Fre et al., 2005, 2009).

Interestingly, in studies on the postnatal developing gut in the mouse or on various organs of amphibians during TH-dependent

[1]Centre de Génétique et de Physiologie Moléculaire et Cellulaire, Université Claude Bernard Lyon 1, 16 Rue Raphael Dubois, Villeurbanne 69622, France. [2]Laboratoire de Biologie Moléculaire de la cellule, Ecole Normale Supérieure de Lyon, 46 Allée d'Italie, Lyon 69007, France.
*Present address: Telethon Institute of Genetics and Medicine (TIGEM), via Campi Flegrei 34, Pozzuoli 80078, Italy. ‡Present address: Centre de Recherche en Cancérologie de Lyon (CRCL), 28 Rue Laennec, Lyon 69373, France.
§These authors contributed equally to this work

¶Author for correspondence (michelina.plateroti@univ-lyon1.fr)

Received 12 January 2015; Accepted 10 July 2015

Development (2015) 142, 2764-2774 doi:10.1242/dev.121962

metamorphosis, TH signaling has been shown to control several components of the Notch pathway (Kress et al., 2009; Buchholz et al., 2007; Mukhi and Brown, 2011; Sun et al., 2013; Das et al., 2006). However, it is not clear whether this control results in Notch activation, and the mechanisms of such regulation and its biological significance have remained largely unknown. Using cellular and molecular approaches in both *in vivo* and *in vitro* systems, we show here that TH, via the TRα1 nuclear receptor, positively modulates the Notch pathway in mouse intestinal crypts. This control is responsible for balanced epithelial differentiation and finally for correct development and homeostasis of this tissue.

RESULTS

THs activate the Notch pathway *in vivo* and *in vitro*

To test whether THs could modulate the Notch pathway, we used *Hes1*-EmGFP^{SAT} Notch-reporter mice (Fre et al., 2011b) to analyze the responsiveness of the transgene to alterations in TH levels. Notably, GFP expression in these mice mirrors that of *Hes1*, a known Notch target gene. Interestingly, we observed a significant increase in GFP expression at both the mRNA and protein levels in TH-injected reporter mice compared with untreated animals (Fig. 1A,B).

To monitor the responsiveness *in vitro* to TH-TRα1, we used a Notch-responsive luciferase reporter system containing RBP-J binding sites (Peignon et al., 2011). These experiments were performed in Cos7 and Caco2 cell lines in which RBP-J-luc was transfected together with the Notch1 intracellular domain (NICD) and TRα1 alone or in combination. For each condition, the cells were maintained in T3-depleted serum with and without the addition of T3 (Fig. 1C). As expected, in both cell lines transfected only with the RBP-J-luc vector (the control condition), T3 treatment failed to have an effect compared with untreated cells. Cells transfected with NICD alone (considered to be the positive control) showed a strong and significant increase in luciferase activity compared with untreated cells. Moreover, whereas Cos7 cells were unresponsive to T3 treatment because of the absence of TR expression in these cells, Caco2 cells expressing TRα1 (Matosin-Matekalo et al., 1999) showed a significant increase in luciferase activity upon T3 treatment (Fig. 1C). In both cell lines transfected with TRα1, T3 treatment significantly induced luciferase activity compared with untreated cells. Finally, and intriguingly, when cells were co-transfected with TRα1 and NICD, we observed a further significant increase in luciferase activity when compared with the NICD-transfected cells. The addition of T3 to the culture medium significantly further induced luciferase activity compared with untreated cells. This same trend of RBP-J-luciferase activity co-regulation by TRα1 and NICD was confirmed in cells maintained in culture medium containing untreated serum and hence physiological levels of THs (Samuels et al., 1979) (supplementary material Fig. S1). Finally, we also co-transfected both cell lines with a Tcf7l2 dominant negative expression vector (indicated as Tcf4DN) and excluded any involvement of the Wnt pathway in the T3-TRα1-dependent response of Notch activity *in vitro* (supplementary material Fig. S1).

Several components of the Notch pathway respond to TH treatment *in vivo* and display epithelial cell-autonomous regulation

According to the literature, several Notch components are expressed in the intestinal epithelium (Sander and Powell, 2004; Schröder and Gossler, 2002). We investigated their expression by RT-qPCR in the whole intestinal mucosa from 1-month-old wild-type (WT) and TRα$^{0/0}$ mice, which are devoid of all isoforms produced from the *Thra* locus (Gauthier et al., 2001). The mRNA levels of *Notch1* and its target *Hes1* significantly increased upon TH treatment in WT animals (Fig. 2A,B). These data confirm the observations described above for *Hes1*-EmGFP^{SAT} reporter mice. *Notch2* mRNA levels, however, did not change upon TH injection into WT animals (supplementary material Fig. S2A). We completed our analysis by verifying the expression of Notch ligands, including Jag1, Jag2, Dll1 and Dll4. We observed a strong and significant increase in

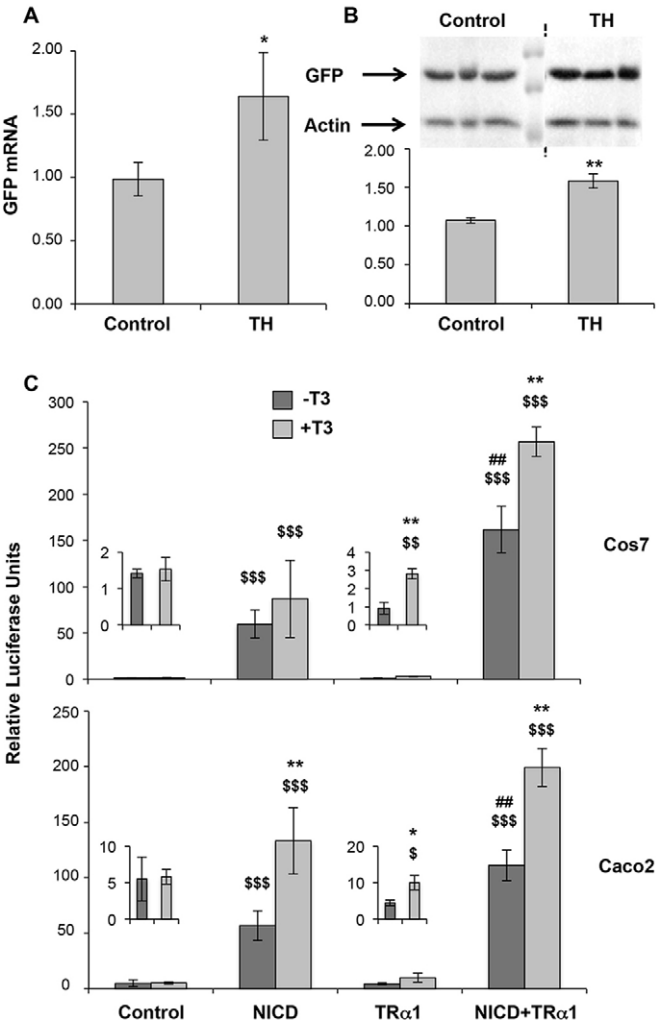

Fig. 1. Notch activity can be modulated by TH-TRα1 *in vivo* and *in vitro*. (A,B) *Hes1*-EmGFP^{SAT} Notch-reporter mice were treated, or otherwise, with TH, and GFP expression was analyzed. (A) RT-qPCR study of *GFP* mRNA expression levels (after normalization with *Ppib*) in the intestine. n=4; *P<0.05, compared with the untreated animals. (B) (Top) Western blot analysis of GFP protein levels in the intestines of three animals per condition. Actin was used as a loading control. (Bottom) GFP levels as obtained by densitometry analysis (ImageJ) and normalized to actin. n=3; *P<0.01, compared with the untreated animals. Dotted black line indicates a cut and junction of two parts of the same membrane. (C) The RBP-J-luciferase reporter was transfected into Cos7 cells (top) or Caco2 cells (bottom) alone (Control) or together with TRα1 and/or NICD expression vectors, as indicated, in the absence or presence of T3. Pictures are representative of two independent experiments each conducted on six replicates. n=6; *P<0.05 and **P<0.01 compared with the untreated condition (–T3); $^{\$}P$<0.05, $^{\$\$}P$<0.01 and $^{\$\$\$}P$<0.001 compared with the control condition; $^{\#\#}P$<0.01 compared with the NICD condition. All bar charts show mean±s.d. The small inset bar charts above Control and TRa1 conditions show the data on different scales.

Development (2015) 142, 2764-2774 doi:10.1242/dev.121962

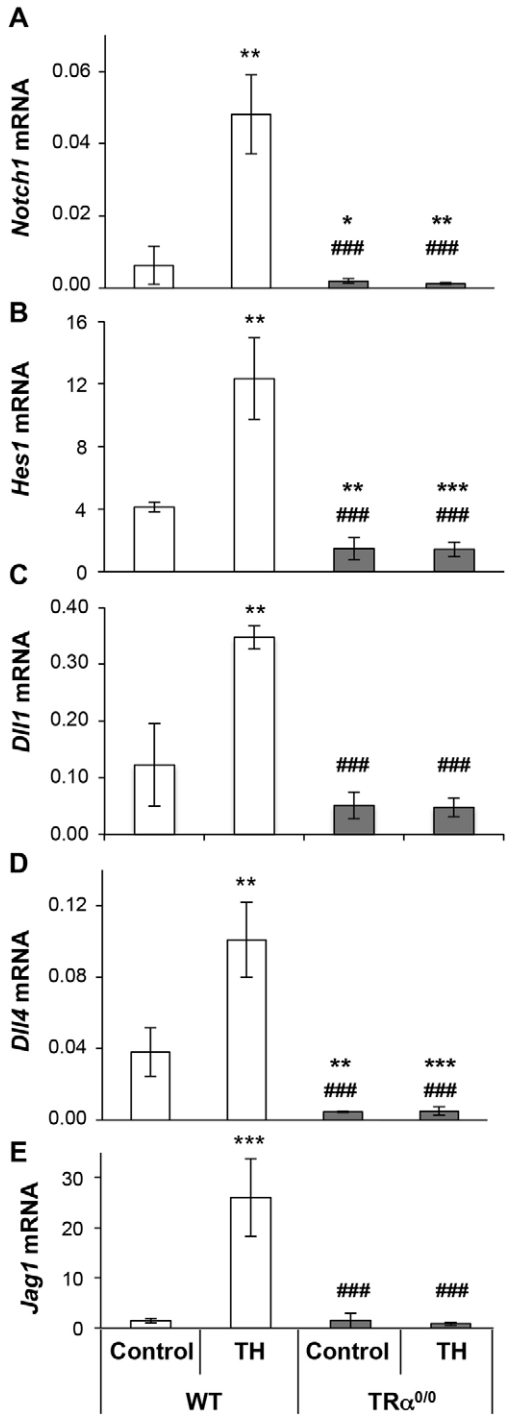

Fig. 2. THs activate mRNA expression of several components of the Notch pathway in the intestine via the *Thra* gene. RT-qPCR experiments were performed to analyze the expression of *Notch1* (A), *Hes1* (B), *Dll1* (C), *Dll4* (D) and *Jag1* (E) in WT (white bars) and TRα$^{0/0}$ (gray bars) animals treated, or otherwise, with TH as indicated. Expression has been normalized to *Ppib*. Mean±s.d.; n=3. *P<0.05, **P<0.01 and ***P<0.001 compared with the WT control animals; $^{###}P$<0.001 compared with the TH-treated WT animals.

Jag1, *Dll1* and *Dll4* mRNAs upon TH treatment of WT mice (Fig. 2C-E), whereas no differences were observed for *Jag2* mRNA (supplementary material Fig. S2B). Interestingly, in TRα$^{0/0}$ animals there was no response to TH treatment for the entire set of genes analyzed, and their overall expression levels in the control condition were significantly lower than those in the WT (Fig. 2). These results clearly indicate that TRα1 is the T3 receptor involved in the modulation of the genes analyzed, in accord with its major role in crypt cell physiology (Plateroti et al., 1999) and with its expression domain (supplementary material Fig. S3).

We used an intestinal epithelial primary culture approach to evaluate whether *Notch1*, *Hes1*, *Jag1*, *Dll1* and *Dll4* mRNA levels were regulated by T3 in an epithelium-autonomous manner. The cells were treated, or otherwise, with T3 for 6 h (early responsiveness) or 24 h (late responsiveness). *Notch1* mRNA levels did not change in T3-treated compared with untreated cells (Fig. 3A), in contrast to the increase observed in TH-treated animals. The lack of *Notch1* mRNA induction by T3 in isolated epithelial cells suggests that complex cell-cell interactions (i.e. epithelial-mesenchymal interactions; reviewed by Kedinger et al., 1998) might be responsible for its stimulation in the whole mucosa. By contrast, *Hes1*, *Dll1* and *Dll4* mRNAs were upregulated by 24 h T3 treatment but were not affected by short-term T3 treatment (Fig. 3B-D). Interestingly, *Jag1* mRNA expression was significantly increased in primary cultures after both short-term and long-term T3 treatment (Fig. 3E).

TRα1 binds to the *Jag1* promoter *in vitro* and *in vivo*

To investigate whether *Dll1*, *Dll4*, *Hes1* and *Jag1* might be transcriptional targets of TRα1, we used Nubiscan software (http://www.nubiscan.unibas.ch) to search *in silico* for putative TRα1 binding sites (TREs) within these genes. However, in accordance with its early T3 responsiveness, we could map potential TREs (TRE1, 2 and 3) only within the *Jag1* promoter (supplementary material Fig. S4A), and these TREs were subsequently investigated for TRα1 binding *in vitro* by EMSA. We observed that TRα1 binds to TRE1 and TRE3 (supplementary material Fig. S4B), and could exclude specific TRα1 binding to TRE1 on chromatin *in vivo* (Fig. 4A). Thus, for in-depth EMSA analyses we focused on TRE3 (hereafter termed *Jag1*-TRE3) (supplementary material Fig. S5). TRα1 binds to this site as a monomer, as a homodimer or as a heterodimer in combination with its physiological partner RXRα (supplementary material Fig. S5A), as expected from the literature (Oetting and Yen, 2007), similar to the well-characterized *Ctnnb1*-TRE (supplementary material Fig. S5C) (Plateroti et al., 2006). The binding can be outcompeted with an excess of cold probe and can be supershifted by adding an anti-TRα1 antibody (supplementary material Fig. S5A,C). Finally, TRα1 could not bind a mutated version of the *Jag1*-TRE3 sequence (supplementary material Fig. S5B).

To confirm that TRα1 can bind the *Jag1*-TRE3 *in vivo*, we used a ChIP approach. The ChIP assay was performed on fresh epithelial preparations from WT mouse intestine using anti-TRα1, anti-TRβ1 or rabbit IgG (negative control). As shown in Fig. 4A, TRα1, but not TRβ1, bound to the *Jag1* promoter region containing the *Jag1*-TRE3 site but did not bind to the TRE1 sequence that is located 3 kb upstream of *Jag1*-TRE3. The percentage of TRα1 binding *in vivo* was similar to that previously described for *Sfrp2*-TRE (Kress et al., 2009) or *Ctnnb1*-TRE (Plateroti et al., 2006) (Fig. 4A); no specific binding was detected on the villin 1 (Vil1) or *Rplp0* gene promoters (Fig. 4A). Interestingly, when we compared the human and mouse *Jag1* genes using the VISTA browser (http://pipeline.lbl.gov/cgi-bin/gateway2), the *Jag1*-TRE3 site was the only conserved element among the three TREs identified by Nubiscan (Fig. 4B).

Jag1 expression pattern in intestinal crypts

The pattern of *Jag1* mRNA expression in intestinal crypts has been investigated previously (Sander and Powell, 2004). However, we

Development (2015) 142, 2764-2774 doi:10.1242/dev.121962

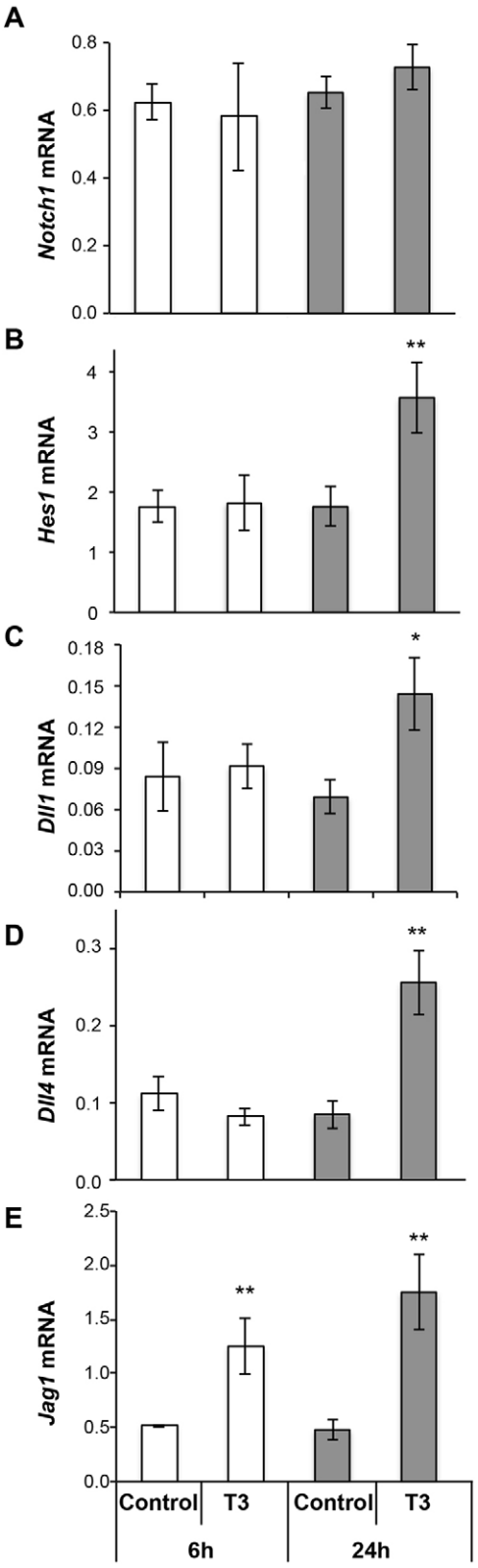

Fig. 3. Intestinal epithelial cell-autonomous response to TH. Intestinal epithelial primary cultures were used to analyze by RT-qPCR the mRNA levels of *Notch1* (A), *Hes1* (B), *Dll1* (C), *Dll4* (D) and *Jag1* (E). Cells were maintained in control conditions or treated with T3 for 6 h (white bars) or 24 h (gray bars). Expression has been normalized to *Ppib*. Results are representative of two independent experiments, each conducted in triplicate. Mean±s.d.; n=3. *P<0.05 and **P<0.01 compared with the respective control condition.

have only limited information with respect to its expression at the protein level in different crypt cell populations (precursors versus Paneth cells). We took advantage of *Hes1*-EmGFP^{SAT} Notch-reporter mice and used an *in toto* crypt immunolabeling protocol (Bellis et al., 2012) to perform multiple immunostainings. This allowed us to analyze the relationship between Jag1-expressing cells and GFP/Hes1-positive cells (i.e. stem and absorptive progenitor cells; Fre et al., 2011b), Dll1-expressing secretory progenitor cells (van Es et al., 2012) and lysozyme-expressing Paneth cells (Fig. 5).

Interestingly, two different pools of crypt cells were positive for Jag1 at the level of the basal and lateral membranes (Fig. 5A,B). One pool was located in the superior portion of the crypts adjacent or corresponding to GFP/Hes1-expressing cells (Fig. 5A, high magnification). The other pool was located at the crypt bottom adjacent to GFP/Hes1-positive cells, which correspond to the columnar basal stem cells (CBCs) (Fre et al., 2011b) (Fig. 5B, high magnification). Interestingly, we observed a partial overlap between Jag1-positive and Dll1-positive cells (supplementary material Fig. S6), with some cells clearly expressing Dll1 only (supplementary material Fig. S6B). It is worth noting that the GFP/Hes1-positive cells also expressed the Ki67 proliferation marker (supplementary material Fig. S7A), further confirming that these cells are precursors (progenitors and stem cells). Moreover, combining GFP/Hes1, Jag1 and lysozyme immunolabeling, we observed that GFP/Hes1 staining did not colocalize with lysozyme, confirming that the GFP/Hes1-expressing cells at the crypt bottom are indeed the CBCs (Fre et al., 2011b) (Fig. 5A-C; supplementary material Movie 1). In this same subcompartment, Jag1 staining appears to be present between lysozyme-expressing Paneth cells and GFP/Hes1-expressing CBCs (Fig. 5A-C; supplementary material Movies 2 and 3).

The same immunolabeling approach in TRα$^{0/0}$ crypts did not allow visualization of Jag1 protein because of the very low expression level. In addition, it did not reveal any qualitative differences in Jag1 staining between *Hes1*-EmGFP^{SAT} mice injected, or otherwise, with TH (not shown). However, increased levels of Jag1 protein were observed by western blot in WT animals injected with TH (supplementary material Fig. S8).

The *Thra* gene controls balanced intestinal epithelial differentiation

Our previous observations of TRα$^{0/0}$ animals indicated a strong defect in intestinal crypt cell proliferation, causing a shortening of the crypt-villus axis compared with age-matched WT animals (Gauthier et al., 2001; Plateroti et al., 2001). However, we had little data about cell type differentiation. To link TH-TRα1 action on Notch activity with its relevance in intestinal physiology, we investigated in more detail the balance between cell proliferation and cell differentiation in 1-month-old WT and TRα$^{0/0}$ mice in both the proximal jejunum and the distal ileum (Fig. 6; supplementary material Fig. S9).

First, we confirmed the reduced number of epithelial cells and the reduced rate of crypt cell proliferation in TRα$^{0/0}$ mice compared with WT animals (supplementary material Fig. S9A,B). Next, by focusing on the differentiation capacities of the major epithelial cell types, we found unbalanced absorptive versus secretory cell type differentiation in TRα$^{0/0}$ animals. The percentage of alkaline phosphatase-expressing absorptive cells (enterocytes) was significantly decreased, and a significant overall increase was observed in the number of both secretory lysozyme-positive (Paneth) and periodic acid-Schiff (PAS)-stained (goblet) cells in TRα$^{0/0}$ compared with WT animals (Fig. 6A,B; supplementary

Development (2015) 142, 2764-2774 doi:10.1242/dev.121962

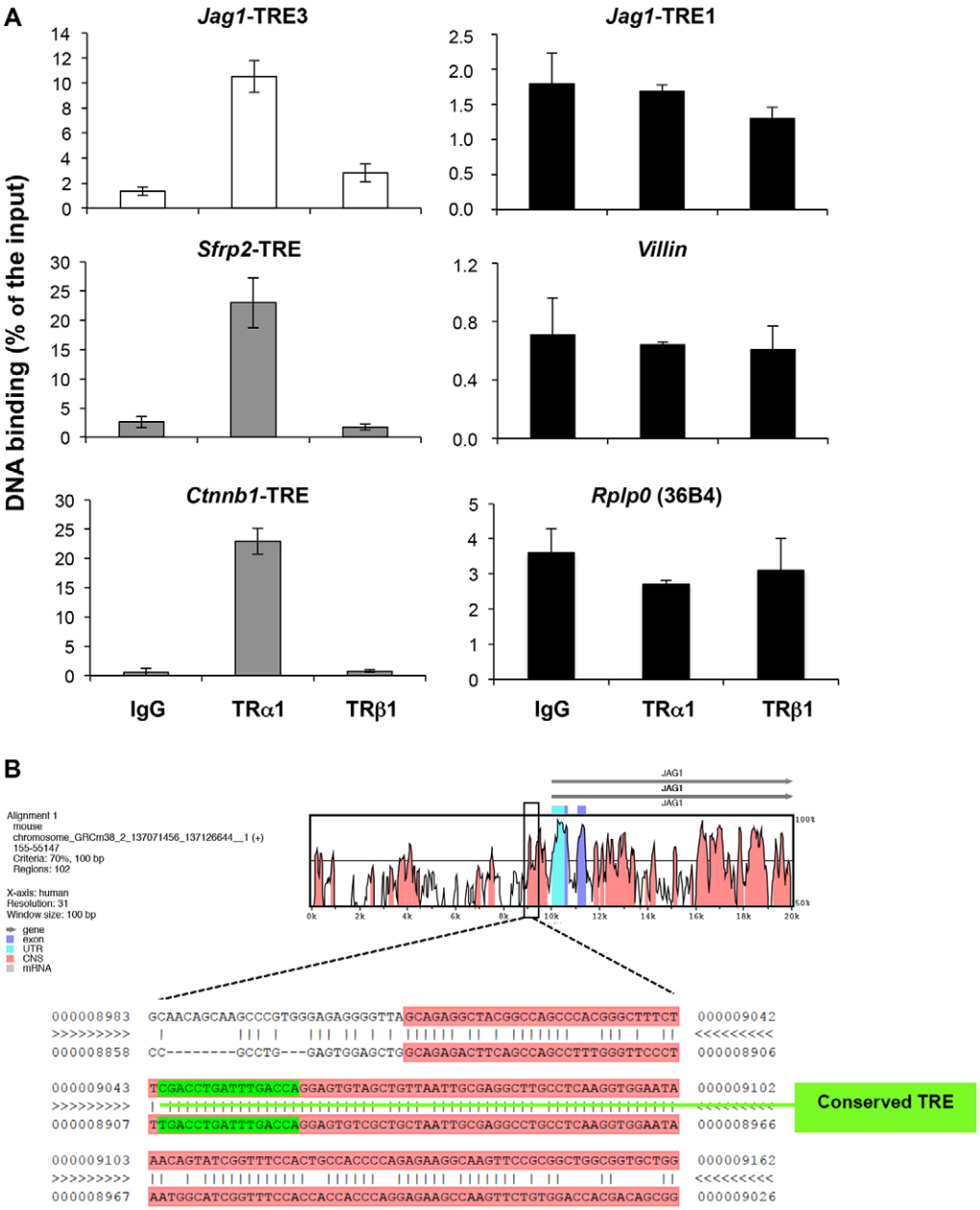

Fig. 4. Chromatin occupancy by TRα1 on the conserved *Jag1*-TRE3. (A) ChIP analysis was performed with chromatin isolated from freshly prepared intestinal epithelial cells from WT mice and immunoprecipitated with anti-TRα1, anti-TRβ1 or rabbit IgG (negative control). qPCR was performed using specific primers covering the *Jag1*-TRE3 and the *Sfrp2*-TRE or the *Ctnnb1*-TRE (positive controls). Non-specific enrichment of TRα1 was evaluated on *Jag1*-TRE1, and on the Vil1 (villin 1) and *Rplp0* (*36B4*) promoters (negative controls); the *Ppia* gene was used as an internal control. Mean±s.d. (n=3) of the specific DNA enrichment in each sample immunoprecipitated with the indicated antibody, expressed as a percentage of the starting input. (B) Alignment of human *JAG1* and mouse *Jag1* genes, including the respective coding regions and 10 kb of the promoters, by VISTA alignment. The *Jag1*-TRE3 sequence is present in the promoters of both species and is very highly conserved (94%) (bottom panel). Its position in human and mouse is: human TRE, –1532 from ATG, –959 from exon 1; mouse TRE, –1479 from ATG, –1183 from exon 1.

material Fig. S9C,E). The percentage of secretory chromogranin A-positive cells (enteroendocrine) was increased in both the proximal jejunum and the distal ileum, but it reached statistical significance only in the latter region (Fig. 6A,B; supplementary material Fig. S9D). RT-qPCR analysis of differentiation markers further confirmed the results obtained by immunochemical or histochemical staining (supplementary material Fig. S10). In summary, these results show a perturbed balance of both cell proliferation and cell differentiation in the intestinal epithelium of $TR\alpha^{0/0}$ animals.

Jag1 links TH-TRα1 and Notch pathway activity in epithelial precursors *in vitro*

Finally, we investigated whether a direct functional link exists between TH-TRα1-dependent *Jag1* regulation and Notch activation in intestinal precursors. We used the intestinal epithelial primary cultures maintained in the control condition or treated with T3 for 24 h alone or together with a Jag1-blocking antibody, or an anti-GFP antibody (considered as negative control). Of note, the anti-Jag1 antibody used specifically recognizes the extracellular epitope that interacts with Notch receptors, blocking their interaction as already described (Saravanamuthu et al., 2009).

Immunolabeling experiments showed the presence of Jag1 essentially in all epithelial cells (Fig. 7A; supplementary material Fig. S11A). At the mRNA level, the treatment with T3 induced the expression of *Jag1* compared with the control condition, and independently of any blocking treatments (supplementary material Fig. S11B). In these same conditions we also analyzed Hes1 expression, which is considered as the readout of Notch activity (Fig. 7B,C; supplementary material Fig. S11B). Interestingly, the cells treated with T3 showed a significant increase in the percentage of nuclei expressing Hes1 compared with control cells. However, in cells co-treated with T3 and the anti-Jag1 antibody this percentage was significantly decreased

Development (2015) 142, 2764-2774 doi:10.1242/dev.121962

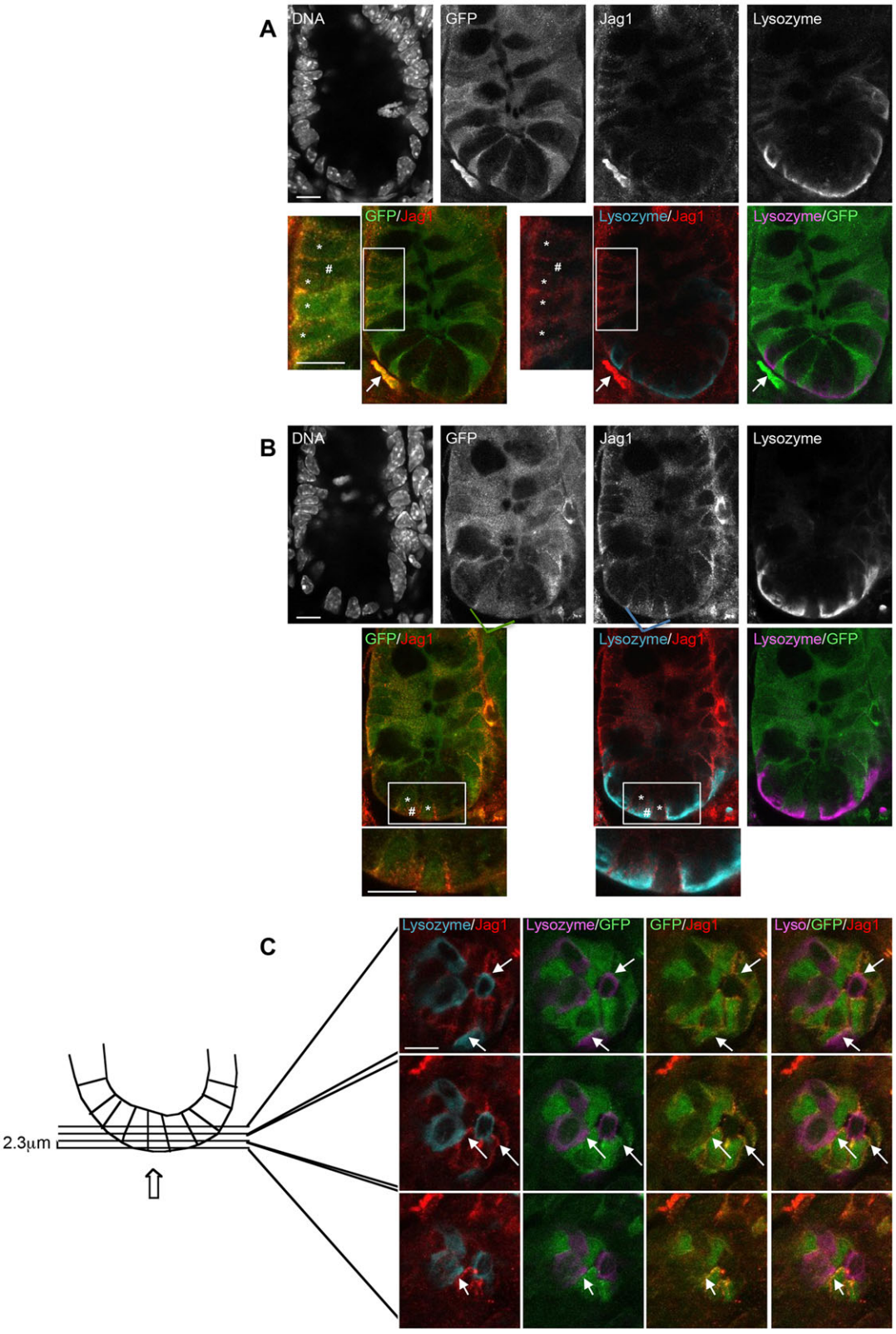

Fig. 5. Pattern of Jag1 expression in the intestinal crypts. (A-C) Whole-crypt immunostaining for Jag1 (red), GFP/Hes1 (green), lysozyme (cyan or magenta) and DNA, as indicated. Images in A and B show maximum intensity projections of three consecutive focal planes (z=0.42 μm). Black and white images in upper panels show each single labeling. Images in C show an intestinal crypt imaged from the bottom; each image represents the maximum intensity projection of five consecutive focal planes (z=0.47 μm). The differences in staining intensity between A and B are due to the different working distances at which the images have been acquired. The arrow in A indicates non-specific staining. Asterisks and hashes in A and B indicate GFP-positive and GFP-negative cells, respectively. The boxed regions are magnified to the left (A) or beneath (B). The arrows in C indicate Jag1 staining between Paneth cells and GFP-expressing cells. Scale bars: 10 μm.

Development (2015) 142, 2764-2774 doi:10.1242/dev.121962

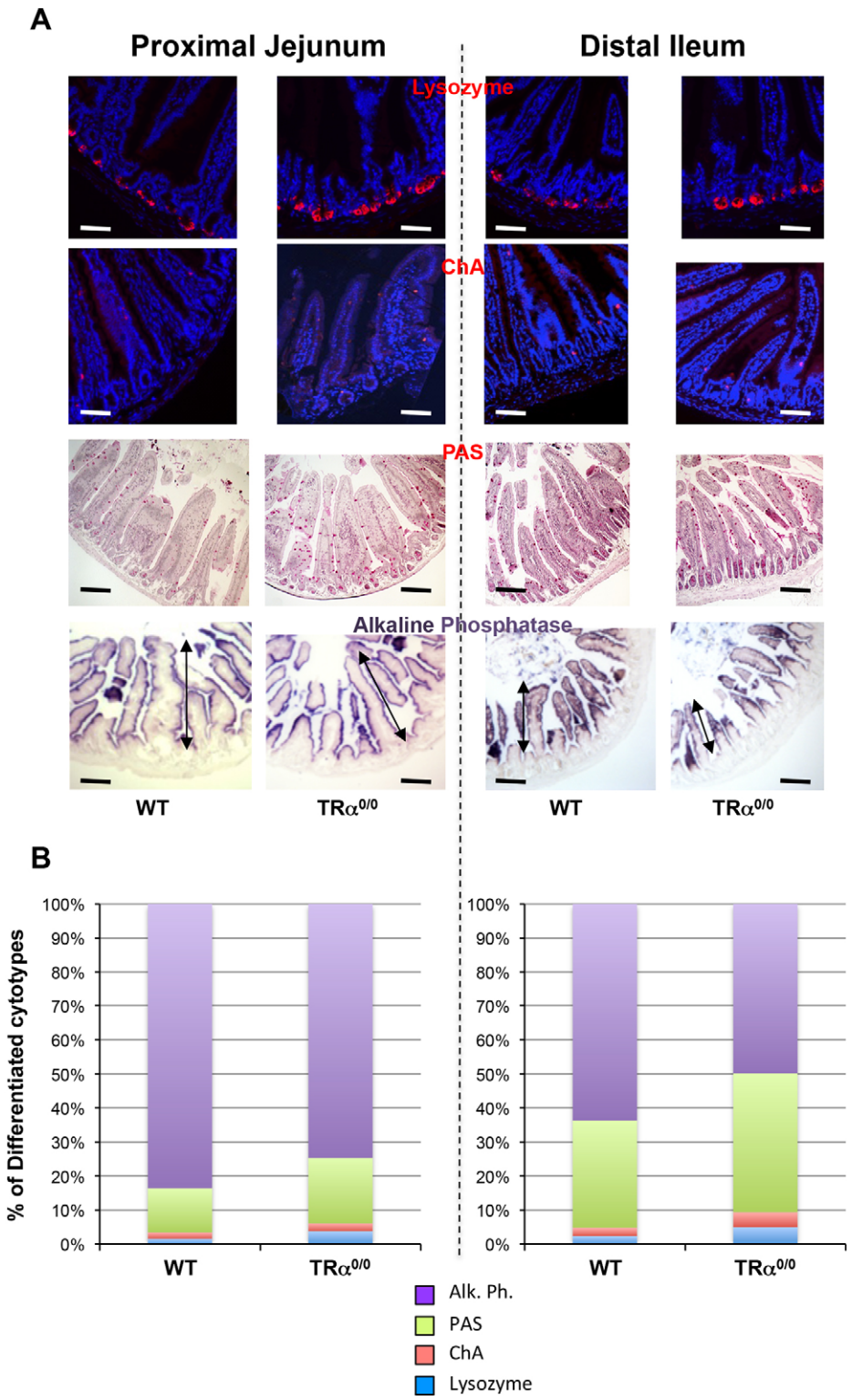

Fig. 6. TRα$^{0/0}$ mice display unbalanced epithelial cell differentiation. (A) Analysis of different differentiation markers in proximal jejunum and distal ileum sections of WT and TRα$^{0/0}$ mice. Lysozyme-positive (Paneth) and chromogranin A (ChA)-positive (enteroendocrine) cells were analyzed by immunolabeling. The images show merged differentiation marker (red) and nuclear staining (blue). Mucus-producing goblet cells were stained with PAS; alkaline phosphatase activity labeled the enterocytes. The double-headed arrow indicates alkaline phosphatase-positive cells per villus axis. Scale bars: 30 µm. (B) Quantification of cells positive for each marker in the crypt-villus axes. Approximately 30 axes were scored under the microscope from at least four mice per genotype; mean values for the percentages of specific cell types are shown.

compared with the T3-treated cells. The action of the anti-Jag1 antibody was specific, given that we did not observe any interference by the anti-GFP antibody (Fig. 7B,C; supplementary material Fig. S11A). The analysis of *Hes1* mRNA levels paralleled the observations of Hes1 immunostaining (Fig. 7B versus supplementary material Fig. S11B); as expected, no differences in *Notch1* mRNA expression were observed in the different culture conditions (supplementary material Fig. S11B).

DISCUSSION

Notch is an evolutionarily conserved and crucial pathway with a pivotal role in cell fate determination in multiple tissues (Artavanis-Tsakonas et al., 1995; Jensen et al., 2000; Fre et al., 2011a). Interestingly, during TH-dependent metamorphosis in *Xenopus laevis*, several components of the Notch pathway are transcriptionally modulated, as observed in newly forming zones of the nervous system corresponding to postnatal neurogenesis (Das

Development (2015) 142, 2764-2774 doi:10.1242/dev.121962

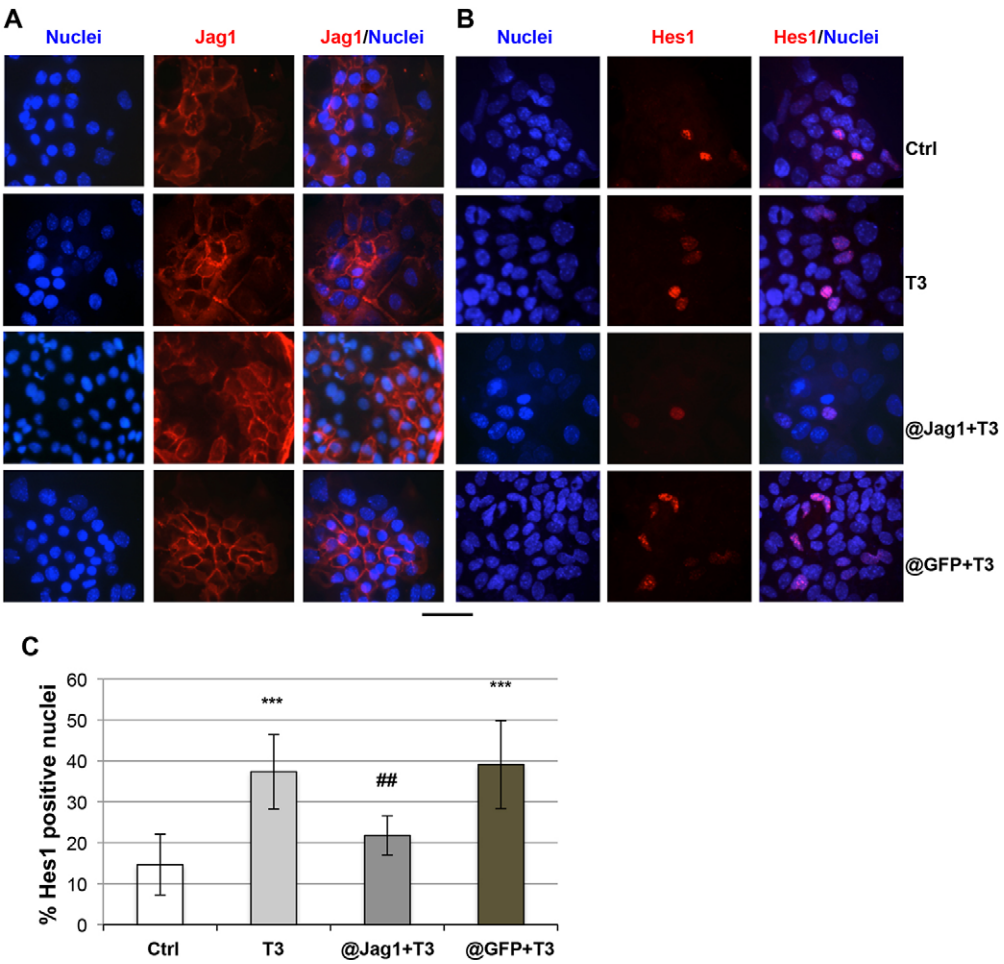

Fig. 7. Functional link between T3-dependent Jag1 expression and Notch pathway activity. (A,B) Jag1 (A) and Hes1 (B) immunolabeling of intestinal epithelial primary cultures maintained in different conditions. Nuclear staining (blue), specific staining (red) and merges are shown. Images are representative of two independent experiments, each conducted in triplicate. Scale bar: 10 µm. (C) Quantification of the percentage of Hes1-positive nuclei. Approximately 15 fields per condition were scored under the microscope; shown in the mean±s.d. ***P<0.001, compared with control; ##P<0.01, compared with T3. Ctrl, Control; T3, 10-7M T3; @Jag1, anti-Jag1 antibody; @GFP, anti-GFP antibody.

et al., 2006) or during the intestinal remodeling that occurs when the animal adapts from a vegetarian to a carnivorous diet (Das et al., 2006). In both cases, however, no in-depth analysis has been performed to determine the mechanisms of this regulation or its biological significance. We show here that, in the murine intestine, TH signaling through the TRα1 nuclear receptor controls the Notch pathway via complex epithelial cell-autonomous and non-autonomous gene regulation, which also includes direct transcriptional control of the *Jag1* gene. The functional consequence of this complex control is clearly revealed in TRα$^{0/0}$ animals, which display an unbalanced cell fate, in accordance with the well described function of the Notch pathway in intestinal epithelial cell fate determination (reviewed by Fre et al., 2011a; Koch et al., 2013; Noah and Shroyer, 2013; Perdigoto and Bardin, 2013).

Previous findings in inducible animal models highlighted the involvement of Dll1 and Dll4 ligands in modulating Notch activity in the adult intestine (Pellegrinet et al., 2011); in this same setting, Jag1 appeared to play only a marginal role (Pellegrinet et al., 2011). It is worth underlining, however, that this work is based on conditional animal models, and the mutations were induced in the adult intestine and for a limited length of time, which might attenuate the phenotypes. In fact, increased Jag1 expression and its participation in intestinal Notch activity have clearly been established in pathological conditions, such as inflammation or cancer (Imaeda et al., 2011; Rodilla et al., 2009; Dai et al., 2014). Interestingly, *Jag1* responds at the transcriptional level to different stimuli/transcription factors that are important for intestinal development and homeostasis, such as Wnt (Peignon et al., 2011; Rodilla et al., 2009) or HNF1α (D'Angelo et al., 2010). Thus, in the intestinal crypts different signaling pathways converge on *Jag1*, strongly suggesting that changes in its expression levels could represent an early molecular event in developing pathologies. Our data on *Jag1* regulation by TRα1 in this same setting also support this role as a 'molecular sensor' of early pathological events such as crypt hypoplasia (hypothyroidism or the lack of *Thra* gene expression) or crypt hyperplasia (hyperthyroidism or increased TRα1 expression). Finally, the fact that Jag1-blocking antibodies can prevent T3-stimulated Notch pathway activity *in vitro* further confirms that Jag1 could actively participate in Notch activity in intestinal epithelial precursors. We therefore propose a model based upon previous literature (reviewed by Gracz and Magness, 2014; Koo and Clevers, 2014) and our new data, in which Jag1 protein is present at the level of crypt progenitors, both absorptive and secretory, and also eventually in Paneth cells (Fig. 5) and participates in Notch activity. It is worth noting, however, that at the level of resolution of confocal microscopy, it is difficult to make a clear distinction between the membranes of two adjacent cells. This is particularly the case for the Jag1-expressing cells present in the upper position of the crypts close to the GFP/Hes1-expressing cells (Fig. 5A).

As regards TRα1, its expression is restricted to crypt cells, including stem cells (Kress et al., 2010; Plateroti et al., 2006) (supplementary material Fig. S3), and *Notch1* and *Hes1*, described here as TH-responsive genes, are part of the stem cell signature defined by the Lgr5 marker (Muñoz et al., 2012). It is thus reasonable to speculate that, by acting simultaneously on

Development (2015) 142, 2764-2774 doi:10.1242/dev.121962

progenitors and on stem cells (directly or indirectly), TRα1 activates the transcription of *Jag1* and enhances the expression of Dll1 and Dll4 as well as of Notch1, finally resulting in an increase of the Notch target Hes1. TRα1 is expressed not only by most of the crypt cells but also by myofibroblasts and muscle cell layers (supplementary material Fig. S3). This pattern of TRα1 expression can help explain the epithelial cell-autonomous and non-autonomous responses that we observed among the different Notch components analyzed. This observation is also in agreement with recent papers describing epithelial/mesenchymal-dependent Notch activity in developing stomach and gut (Kim et al., 2011; Faure et al., 2015). Thus, we cannot exclude the possibility that Jag1 staining at the basal membrane of crypt cells is of mesenchymal origin. This assumption reinforces the model in which complex cell-cell, including epithelial-mesenchymal, interactions play a pivotal role in gut development and homeostasis (reviewed by Kedinger et al., 1998; De Santa Barbara et al., 2002; Faure and de Santa Barbara, 2011).

Studies in both amphibians and mammals have shown that alterations in TH levels or in TR expression have an effect on cellular responses such as proliferation and apoptosis and on signaling pathways such as BMP, Shh and Wnt. In metamorphosing tadpoles, TH and TRs regulate reciprocally instructive epithelium-mesenchyme interactions by modulating the BMP and Shh pathways (Ishizuya-Oka and Hasebe, 2008). Our own work in the mouse intestine has underlined the complex, multilevel interactions between TRα1 and the Wnt pathway in developmental, homeostatic and pathological conditions (Sirakov et al., 2012; Kress et al., 2010, 2009; Plateroti et al., 2006). In mammalian skin, alterations in TH levels influence the Shh pathway, which in turn controls TH availability (Dentice et al., 2007). Notably, several components of the Notch pathway, including Hes1 and Jag1, have been described as targets of Wnt (Fre et al., 2009; Peignon et al., 2011; Rodilla et al., 2009; Estrach et al., 2006). Given that, in studies involving analysis of the whole mucosa, TRα1 activates the Wnt pathway in intestinal crypts (Plateroti et al., 2006; Kress et al., 2009), we cannot exclude the possibility that some of the responses observed for Notch also depend on Wnt activity. However, the RBP-J-luciferase assay that we performed in cell lines clearly revealed the existence of TH-TRα1-dependent Notch activation that is independent of Wnt.

In conclusion, we report here that TRα1 controls Notch activity in the intestinal epithelium. Importantly, the Notch and Wnt pathways are the driving force behind intestinal epithelium progenitor/stem cell biology. The fact that both are under the influence of the TRα1 nuclear receptor is a novel and important finding. Moreover, when these three signaling pathways are dysregulated, alone or in combination, they trigger and/or enhance intestinal carcinogenesis (Fre et al., 2009; Kress et al., 2010; Peignon et al., 2011; Rodilla et al., 2009). Considering the newly described role of TRα1 in stem cell biology (López-Juárez et al., 2012; Ishizuya-Oka and Shi, 2008) and as a tumor inducer (Kress et al., 2010), the data that we present here offer a new perspective for future investigations aimed at defining TH-TRα1 mechanisms of action.

MATERIALS AND METHODS

Animals and sample preparation

We used 1-month-old TRα$^{0/0}$ (Gauthier et al., 2001), *Hes1*-EmGFP^{SAT} (Fre et al., 2011b) and wild-type animals with appropriate genetic backgrounds. The mouse housing and experimentation were approved by the animal experimental committee of the Ecole Normale Supérieure de Lyon (Lyon, France), the Comités d'Ethique en Experimentation Animale de l'Université de Lyon (C2EA55 and C2EA15; registration number DR2013-55) and in accordance with European legislation on animal care and experimentation.

Hyperthyroidism was induced by intraperitoneal injections (once a day for 2 days) of a mixture of T4 and T3 (2.5 mg/kg T4 and 0.25 mg/kg T3) in 100 µl PBS. Animals were fed with standard mouse chow and had *ad libitum* access to food and drinking water. Mice were euthanized at the indicated ages, the intestine was quickly removed, and samples were fixed in 4% paraformaldehyde (PFA) for histological and immunohistochemical experiments or frozen in liquid nitrogen and used for protein and/or RNA extraction. The levels of free T3 and T4 were analyzed by a VIDAS enzyme-linked assay kit (Biomerieux).

Primary cell cultures of intestinal epithelial cells

Intestinal epithelial primary cultures were derived from 4- to 6-day-old neonatal mice. Briefly, following sacrifice, the entire small intestine was removed. The epithelium was isolated as intact organoids by enzymatic dissociation using collagenase type XI (Sigma) and dispase (Boehringer Mannheim) followed by physical disaggregation and filtration on gauze. Organoids were plated in Dulbecco's modified Eagle's medium (DMEM; Invitrogen) supplemented with 2.5% heat-inactivated T3-depleted (Samuels et al., 1979) fetal calf serum (FCS; Life Science), 20 ng/ml epidermal growth factor (Sigma), and insulin-transferrin-selenium diluted 1:100 (Sigma). Culture surfaces were coated with Matrigel Basement Membrane Matrix (BD Biosciences). For treatment experiments, 0.1 µM T3 or vehicle alone was added to the culture medium for the indicated length of time. In contrast to the animal work, only T3 was used to treat cell cultures. The blocking experiments were performed by adding 10 µg/ml anti-Jag1 (R&D Systems, AF599) or anti-GFP (Sigma Aldrich, G1544) antibodies to the culture medium for 48 h.

Immunohistochemistry, histochemistry, histoenzymatic staining and western blotting

Paraffin sections (5 µm thick) were used for indirect immunostaining. Briefly, the sections were deparaffinized in methylcyclohexane, hydrated in ethanol, and washed with PBS. The slides were then subjected to antigen retrieval by heating at 95°C in a microwave in 0.01 M citrate buffer (pH 6), and incubated for 1 h at room temperature with blocking buffer (10% normal goat serum, 1% BSA and 0.02% Triton X-100 in PBS). The slides were incubated with primary antibodies overnight at 4°C followed by incubation with fluorescent secondary antibodies (Jackson Laboratories). All nuclei were stained with Hoechst (Sigma). To label mucus-producing goblet cells, the paraffin sections were subjected to periodic acid-Schiff (PAS) staining as previously reported (Plateroti et al., 1999). Mucin-filled cells were stained in bright fuchsia. Enterocytes were labeled by incubating the sections with the BCIP/NBT (Sigma) alkaline phosphatase substrate. Fluorescence and bright-field microscopy were performed on a Zeiss Z1 imager microscope.

In toto crypt preparation and immunolabeling were performed according to Bellis et al. (2012). Briefly, *Hes1*-EmGFP^{SAT} mice were anaesthetized with a xylazine/ketamine mixture (2 mg/ml xylazine, 40 mg/ml ketamine). The distal part of the small intestine was opened, flushed first with warm (37°C) PHEM buffer (60 mM Pipes, 25 mM Hepes, 10 mM EGTA, 4 mM $MgSO_4$, pH 7.2) and then with a solution of 3% PFA, 0.2% Triton X-100 in PHEM. The intestine was then resected, opened longitudinally, pinned to a wax surface and covered with fixative solution for 1 h at room temperature. Five minutes before the end of the fixation step, the samples were cut into small cubes, and washed three times in PBS for 10 min each. Single rows of crypt-villi were sliced under a stereomicroscope. For immunolabeling, ~40 slices were incubated for 30 min on a rotating wheel at room temperature consecutively in: (1) 200 mM NH_4Cl in PBS; (2) 3% sodium deoxycholate in water; (3) 0.5% Triton X-100 in PBS; and (4) 0.2% Triton X-100, 1% BSA in PBS. All successive incubations and washes used 0.2% Triton X-100, 1% BSA in PBS. The samples were incubated with primary antibodies overnight at 4°C on a rotating wheel, washed three times and incubated with secondary fluorescent antibodies and the DNA dye Hoechst for 6 h at room temperature. Finally, they were washed in PBS before mounting with Mowiol (6 g glycerol, 2.4 g Mowiol 4-88, 6 ml water, 12 ml 0.2 M Tris-Cl pH 8.5 and 1% DABCO). As a control for the specificity of the secondary fluorescent antibodies, primary antibody was omitted. We used the following antibodies: anti-Ki67 (Labvision, RM-9106; 1:100), anti-lysozyme (Abcam, AB108508; 1:500), anti-Jag1 (Santa Cruz, SC-6011;

Development (2015) 142, 2764-2774 doi:10.1242/dev.121962

1:100), anti-Dll1 (Santa Cruz, SC-9102; 1:100), anti-GFP (Millipore, AB16901; 1:350) and anti-chromogranin A (Zymed, 18-0094; 1:50). The secondary antibodies were Alexa Fluor 568 donkey anti-goat, Alexa Fluor 488 goat anti-chicken (Life Technologies, A11057 and A11039; 1:1000) and CFdye 647 donkey anti- rabbit (Biotium, 20047; 1:200).

Confocal microscopy was performed on a Leica SP5X with 63× HC PL APO NA 1.4 oil-immersion objective (Fig. 5A,B) or a Zeiss LSM780 using a 63× AN 1.4 oil-immersion objective (Fig. 5C). Images were processed with ImageJ (NIH) and the 3D reconstruction performed with Imaris 7.6.5 (Bitplane) using the thresholding-based segmentation tool.

Protein extracts from full-thickness mucosa (50 µg/lane) were separated on 8% bis-acrylamide/acrylamide gels and transferred to nitrocellulose membranes (Hybond ECL, Amersham) before saturation and incubation with anti-GFP (Sigma, G1544; 1:1000), anti-Jag1 (Cell Signaling, 2620; 1:250) and anti-actin (Sigma, A5316; 1:10,000) primary antibodies. This step was followed by incubation with HRP-conjugated secondary antibodies (Promega, anti-mouse, W402B, 1:5000; anti-rabbit, W401B, 1:5000; anti-goat, V805A, 1:10,000). The signal was analyzed using an enzymatic chemiluminescence detection kit (LumiLight, Roche).

Cell lines and transfection experiments

This study was performed on the human Caco2 colorectal cancer cell line and on monkey Cos7 cells. Caco2 cells (50,000 cells/well in 24-well plates) and Cos7 cells (30,000 cells/well in 24-well plates) were cultured in DMEM supplemented with 10% and 5% FCS, respectively. We used the following vectors: pRBP-J-luc (200 ng/well) (Peignon et al., 2011), NICD expression vector (100 ng/well) (Peignon et al., 2011) and pGS5-TRα1 (100 ng/well). The vectors were transfected using Exgen transfection reagent (Euromedex). For the T3 treatments, the cells were maintained in TH-depleted serum (Samuels et al., 1979). T3 (1 µM) or vehicle alone was added to the culture medium 24 h before the end of the culture period. Luciferase activity was measured 48 h post-transfection using the Dual-Luciferase Reporter Assay System (Promega).

RNA extraction and analysis

For full-thickness intestinal mucosa samples, RNA was extracted using the RNeasy Kit (Qiagen). Reverse transcription was performed using MuMLV reverse transcriptase (Promega) on 1 µg total RNA according to the manufacturer's instructions and using random hexanucleotide priming (Promega). For primary cultures, RNA was extracted using the Absolutely RNA Nanoprep Kit (Stratagene). Reverse transcription was performed using SuperScript III First-Strand Synthesis SuperMix for qRT-PCR (Invitrogen) on 300 ng total RNA. To avoid the presence of contaminating DNA, DNase digestion was performed on all preparations. All cDNA samples were purified using the the Qiaquick PCR purification kit (Qiagen) before use for qPCR experiments. qPCR analyses were performed with SYBR Green PCR Master Mix (Qiagen) in an MxP3000 apparatus (Stratagene). In each sample, specific mRNA expression was quantified using the standard curve method and values normalized to *Ppib* levels. Primer sequences are listed in supplementary material Table S1A.

Electrophoretic mobility shift assay (EMSA)

Full-length cDNAs for TRα1 and RXRα were transcribed/translated *in vitro* using the Quick TNT Kit (Promega) according to the manufacturer's protocol. The EMSA was performed with radiolabeled probes as previously described (Sirakov et al., 2012). Where indicated, anti-TRα1 antibodies were included in the reaction mix. Probe sequences are listed in supplementary material Table S1C.

Chromatin immunoprecipitation (ChIP) and qPCR analysis

ChIP was performed on epithelial fragments obtained from intestines of 3- to 6-day-old mice after digestion by collagenase/dispase as previously described (Kress et al., 2009). Specific DNA fragments were analyzed by qPCR using the primers listed in supplementary material Table S1B; *Ppia* was used in all reactions as an internal control.

Statistical analysis

Histograms show mean±s.d. Comparisons between groups were performed using Student's *t*-test; $P<0.05$ was considered statistically significant.

Acknowledgements

We thank Professor Spyros Artavanis-Tsakonas (Harvard Medical School, Boston, USA) and Dr Silvia Fre (Institut Curie, Paris, France) for providing the *Hes1*-EmGFP^{SAT} reporter mice; Nadine Aguilera for assistance with animal handling; and Dr Beatrice Romagnolo (Institut Cochin, Paris, France) for providing the pRBP-J-luc and NICD expression vectors.

Competing interests

The authors declare no competing or financial interests.

Author contributions

M.S., conception and design, collection and assembly of data, data analysis and interpretation, manuscript writing; A.B., E.K., C.F. and I.N.L., collection and assembly of data, data analysis and interpretation; J.N., collection and assembly of data; D.A., data analysis and interpretation; M.P., conception and design, assembly of data, data analysis and interpretation, manuscript writing, financial support. All authors approved the manuscript.

Funding

This work was supported by the Agence Nationale de la Recherche (ANR) Blanc ThRaSt [ANR-11-BSV2-019], by the Fondation ARC pour la Recherche sur le Cancer [grant No PGA1201402000834] and by the Département du Rhône de la Ligue contre le cancer [grant No 88283] to M.P.

Supplementary material

Supplementary material available online at
http://dev.biologists.org/lookup/suppl/doi:10.1242/dev.121962/-/DC1

References

Artavanis-Tsakonas, S., Matsuno, K. and Fortini, M. (1995). Notch signaling. *Science* **268**, 225-232.

Barker, N., Bartfeld, S. and Clevers, H. (2010). Tissue-resident adult stem cell populations of rapidly self-renewing organs. *Cell Stem Cell* **7**, 656-670.

Bellis, J., Duluc, I., Romagnolo, B., Perret, C., Faux, M. C., Dujardin, D., Formstone, C., Lightowler, S., Ramsay, R. G., Freund, J.-N. et al. (2012). The tumor suppressor Apc controls planar cell polarities central to gut homeostasis. *J. Cell Biol.* **198**, 331-341.

Buchholz, D. R., Heimeier, R. A., Das, B., Washington, T. and Shi, Y.-B. (2007). Pairing morphology with gene expression in thyroid hormone-induced intestinal remodeling and identification of a core set of TH-induced genes across tadpole tissues. *Dev. Biol.* **303**, 576-590.

Chin, W. W. and Yen, P. M. (1996). T3 or not T3–the slings and arrows of outrageous TR function. *Endocrinology* **137**, 387-388.

Dai, Y., Wilson, G., Huang, B., Peng, M., Teng, G., Zhang, D., Zhang, R., Ebert, M. P. A., Chen, J., Wong, B. C. Y. et al. (2014). Silencing of Jagged1 inhibits cell growth and invasion in colorectal cancer. *Cell Death Dis.* **5**, e1170.

D'Angelo, A., Bluteau, O., Garcia-Gonzalez, M. A., Gresh, L., Doyen, A., Garbay, S., Robine, S. and Pontoglio, M. (2010). Hepatocyte nuclear factor 1alpha and beta control terminal differentiation and cell fate commitment in the gut epithelium. *Development* **137**, 1573-1582.

Das, B., Cai, L., Carter, M. G., Piao, Y.-L., Sharov, A. A., Ko, M. S. H. and Brown, D. D. (2006). Gene expression changes at metamorphosis induced by thyroid hormone in Xenopus laevis tadpoles. *Dev. Biol.* **291**, 342-355.

De Santa Barbara, P., Van Den Brink, G. R. and Roberts, D. J. (2002). Molecular etiology of gut malformations and diseases. *Am. J. Med. Genet.* **115**, 221-230.

Dentice, M., Luongo, C., Huang, S., Ambrosio, R., Elefante, A., Mirebeau-Prunier, D., Zavacki, A. M., Fenzi, G., Grachtchouk, M., Hutchin, M. et al. (2007). Sonic hedgehog-induced type 3 deiodinase blocks thyroid hormone action enhancing proliferation of normal and malignant keratinocytes. *Proc. Natl. Acad. Sci. USA* **104**, 14466-14471.

Estrach, S., Ambler, C. A., Lo Celso, C. L., Hozumi, K. and Watt, F. M. (2006). Jagged 1 is a beta-catenin target gene required for ectopic hair follicle formation in adult epidermis. *Development* **133**, 4427-4438.

Faure, S. and de Santa Barbara, P. (2011). Molecular embryology of the foregut. *J. Pediatr. Gastroenterol. Nutr.* **52** Suppl. 1, S2-S3.

Faure, S., McKey, J., Sagnol, S. and de Santa Barbara, P. (2015). Enteric neural crest cells regulate vertebrate stomach patterning and differentiation. *Development* **142**, 331-342.

Fre, S., Huyghe, M., Mourikis, P., Robine, S., Louvard, D. and Artavanis-Tsakonas, S. (2005). Notch signals control the fate of immature progenitor cells in the intestine. *Nature* **435**, 964-968.

Fre, S., Pallavi, S. K., Huyghe, M., Laé, M., Janssen, K.-P., Robine, S., Artavanis-Tsakonas, S. and Louvard, D. (2009). Notch and Wnt signals cooperatively control cell proliferation and tumorigenesis in the intestine. *Proc. Natl. Acad. Sci. USA* **106**, 6309-6314.

Fre, S., Bardin, A., Robine, S. and Louvard, D. (2011a). Notch signaling in intestinal homeostasis across species: the cases of Drosophila, Zebrafish and the mouse. *Exp. Cell Res.* **317**, 2740-2747.

Fre, S., Hannezo, E., Sale, S., Huyghe, M., Lafkas, D., Kissel, H., Louvi, A., Greve, J., Louvard, D. and Artavanis-Tsakonas, S. (2011b). Notch lineages and activity in intestinal stem cells determined by a new set of knock-in mice. *PLoS ONE* **6**, e25785.

Gauthier, K., Plateroti, M., Harvey, C. B., Williams, G. R., Weiss, R. E., Refetoff, S., Willott, J. F., Sundin, V., Roux, J.-P., Malaval, L. et al. (2001). Genetic analysis reveals different functions for the products of the thyroid hormone receptor alpha locus. *Mol. Cell. Biol.* **21**, 4748-4760.

Gracz, A. D. and Magness, S. T. (2014). Defining hierarchies of stemness in the intestine: evidence from biomarkers and regulatory pathways. *Am. J. Physiol. Gastrointest. Liver Physiol.* **307**, G260-G273.

Horvay, K. and Abud, H. E. (2013). Regulation of intestinal stem cells by Wnt and Notch signalling. *Adv. Exp. Med. Biol.* **786**, 175-186.

Imaeda, H., Andoh, A., Aomatsu, T., Uchiyama, K., Bamba, S., Tsujikawa, T., Naito, Y. and Fujiyama, Y. (2011). Interleukin-33 suppresses Notch ligand expression and prevents goblet cell depletion in dextran sulfate sodium-induced colitis. *Int. J. Mol. Med.* **28**, 573-578.

Ishizuya-Oka, A. and Hasebe, T. (2008). Sonic hedgehog and bone morphogenetic protein-4 signaling pathway involved in epithelial cell renewal along the radial axis of the intestine. *Digestion* **77** Suppl 1, 42-47.

Ishizuya-Oka, A. and Shi, Y.-B. (2008). Thyroid hormone regulation of stem cell development during intestinal remodeling. *Mol. Cell. Endocrinol.* **288**, 71-78.

Jensen, J., Pedersen, E. E., Galante, P., Hald, J., Heller, R. S., Ishibashi, M., Kageyama, R., Guillemot, F., Serup, P. and Madsen, O. D. (2000). Control of endodermal endocrine development by Hes-1. *Nat. Genet.* **24**, 36-44.

Kedinger, M., Duluc, I., Fritsch, C., Lorentz, O., Plateroti, M. and Freund, J. N. (1998). Intestinal epithelial-mesenchymal cell interactions. *Ann. N. Y. Acad. Sci.* **859**, 1-17.

Kim, T.-H., Kim, B.-M., Mao, J., Rowan, S. and Shivdasani, R. A. (2011). Endodermal Hedgehog signals modulate Notch pathway activity in the developing digestive tract mesenchyme. *Development* **138**, 3225-3233.

Koch, U., Lehal, R. and Radtke, F. (2013). Stem cells living with a Notch. *Development* **140**, 689-704.

Koo, B.-K. and Clevers, H. (2014). Stem cells marked by the R-spondin receptor LGR5. *Gastroenterology* **147**, 289-302.

Kress, E., Rezza, A., Nadjar, J., Samarut, J. and Plateroti, M. (2009). The frizzled-related sFRP2 gene is a target of thyroid hormone receptor alpha1 and activates beta-catenin signaling in mouse intestine. *J. Biol. Chem.* **284**, 1234-1241.

Kress, E., Skah, S., Sirakov, M., Nadjar, J., Gadot, N., Scoazec, J.-Y., Samarut, J. and Plateroti, M. (2010). Cooperation between the thyroid hormone receptor TRalpha1 and the WNT pathway in the induction of intestinal tumorigenesis. *Gastroenterology* **138**, 1863-1874.e1.

López-Juárez, A., Remaud, S., Hassani, Z., Jolivet, P., Pierre Simons, J., Sontag, T., Yoshikawa, K., Price, J., Morvan-Dubois, G. and Demeneix, B. A. (2012). Thyroid hormone signaling acts as a neurogenic switch by repressing Sox2 in the adult neural stem cell niche. *Cell Stem Cell* **10**, 531-543.

Matosin-Matekalo, M., Mesonero, J. E., Laroche, T. J., Lacasa, M. and Brot-Laroche, E. (1999). Glucose and thyroid hormone co-regulate the expression of the intestinal fructose transporter GLUT5. *Biochem. J.* **339**, 233-239.

Mukhi, S. and Brown, D. D. (2011). Transdifferentiation of tadpole pancreatic acinar cells to duct cells mediated by Notch and stromelysin-3. *Dev. Biol.* **351**, 311-317.

Muñoz, J., Stange, D. E., Schepers, A. G., van de Wetering, M., Koo, B.-K., Itzkovitz, S., Volckmann, R., Kung, K. S., Koster, J., Radulescu, S. et al. (2012). The Lgr5 intestinal stem cell signature: robust expression of proposed quiescent '+4' cell markers. *EMBO J.* **31**, 3079-3091.

Noah, T. K. and Shroyer, N. F. (2013). Notch in the intestine: regulation of homeostasis and pathogenesis. *Annu. Rev. Physiol.* **75**, 263-288.

Oetting, A. and Yen, P. M. (2007). New insights into thyroid hormone action. *Best Pract. Res. Clin. Endocrinol. Metab.* **21**, 193-208.

Peignon, G., Durand, A., Cacheux, W., Ayrault, O., Terris, B., Laurent-Puig, P., Shroyer, N. F., Van Seuningen, I., Honjo, T., Perret, C. et al. (2011). Complex interplay between beta-catenin signalling and Notch effectors in intestinal tumorigenesis. *Gut* **60**, 166-176.

Pellegrinet, L., Rodilla, V., Liu, Z., Chen, S., Koch, U., Espinosa, L., Kaestner, K. H., Kopan, R., Lewis, J. and Radtke, F. (2011). Dll1- and dll4-mediated notch signaling are required for homeostasis of intestinal stem cells. *Gastroenterology* **140**, 1230-1240 e1231-1237.

Perdigoto, C. N. and Bardin, A. J. (2013). Sending the right signal: Notch and stem cells. *Biochim. Biophys. Acta* **1830**, 2307-2322.

Plateroti, M., Chassande, O., Fraichard, A., Gauthier, K., Freund, J., Samarut, J. and Kedinger, M. (1999). Involvement of T3Ralpha- and beta-receptor subtypes in mediation of T3 functions during postnatal murine intestinal development. *Gastroenterology* **116**, 1367-1378.

Plateroti, M., Gauthier, K., Domon-Dell, C., Freund, J.-N., Samarut, J. and Chassande, O. (2001). Functional interference between thyroid hormone receptor alpha (TRalpha) and natural truncated TRDeltaalpha isoforms in the control of intestine development. *Mol. Cell. Biol.* **21**, 4761-4772.

Plateroti, M., Kress, E., Mori, J. I. and Samarut, J. (2006). Thyroid hormone receptor alpha1 directly controls transcription of the beta-catenin gene in intestinal epithelial cells. *Mol. Cell. Biol.* **26**, 3204-3214.

Radtke, F., Clevers, H. and Riccio, O. (2006). From gut homeostasis to cancer. *Curr. Mol. Med.* **6**, 275-289.

Riccio, O., van Gijn, M. E., Bezdek, A. C., Pellegrinet, L., van Es, J. H., Zimber-Strobl, U., Strobl, L. J., Honjo, T., Clevers, H. and Radtke, F. (2008). Loss of intestinal crypt progenitor cells owing to inactivation of both Notch1 and Notch2 is accompanied by derepression of CDK inhibitors p27Kip1 and p57Kip2. *EMBO Rep.* **9**, 377-383.

Robinson-Rechavi, M., Escriva Garcia, H. and Laudet, V. (2003). The nuclear receptor superfamily. *J. Cell Sci.* **116**, 585-586.

Rodilla, V., Villanueva, A., Obrador-Hevia, A., Robert-Moreno, A., Fernández-Majada, V., Grilli, A., López-Bigas, N., Bellora, N., Albà, M. M., Torres, F. et al. (2009). Jagged1 is the pathological link between Wnt and Notch pathways in colorectal cancer. *Proc. Natl. Acad. Sci. USA* **106**, 6315-6320.

Samuels, H. H., Stanley, F. and Casanova, J. (1979). Depletion of L-3,5,3′-triiodothyronine and L-thyroxine in euthyroid calf serum for use in cell culture studies of the action of thyroid hormone. *Endocrinology* **105**, 80-85.

Sancho, R., Cremona, C. A. and Behrens, A. (2015). Stem cell and progenitor fate in the mammalian intestine: Notch and lateral inhibition in homeostasis and disease. *EMBO Rep.* **16**, 571-581.

Sander, G. R. and Powell, B. C. (2004). Expression of notch receptors and ligands in the adult gut. *J. Histochem. Cytochem.* **52**, 509-516.

Saravanamuthu, S. S., Gao, C. Y. and Zelenka, P. S. (2009). Notch signaling is required for lateral induction of Jagged1 during FGF-induced lens fiber differentiation. *Dev. Biol.* **332**, 166-176.

Schröder, N. and Gossler, A. (2002). Expression of Notch pathway components in fetal and adult mouse small intestine. *Gene Expr. Patterns* **2**, 247-250.

Shi, Y.-B., Hasebe, T., Fu, L., Fujimoto, K. and Ishizuya-Oka, A. (2011). The development of the adult intestinal stem cells: Insights from studies on thyroid hormone-dependent amphibian metamorphosis. *Cell Biosci.* **1**, 30.

Sirakov, M. and Plateroti, M. (2011). The thyroid hormones and their nuclear receptors in the gut: from developmental biology to cancer. *Biochim. Biophys. Acta* **1812**, 938-946.

Sirakov, M., Skah, S., Lone, I. N., Nadjar, J., Angelov, D. and Plateroti, M. (2012). Multi-level interactions between the nuclear receptor TRalpha1 and the WNT effectors beta-catenin/Tcf4 in the intestinal epithelium. *PLoS ONE* **7**, e34162.

Stappenbeck, T. S., Wong, M. H., Saam, J. R., Mysorekar, I. U. and Gordon, J. I. (1998). Notes from some crypt watchers: regulation of renewal in the mouse intestinal epithelium. *Curr. Opin. Cell Biol.* **10**, 702-709.

Sun, G., Heimeier, R. A., Fu, L., Hasebe, T., Das, B., Ishizuya-Oka, A. and Shi, Y.-B. (2013). Expression profiling of intestinal tissues implicates tissue-specific genes and pathways essential for thyroid hormone-induced adult stem cell development. *Endocrinology* **154**, 4396-4407.

van der Flier, L. G. and Clevers, H. (2009). Stem cells, self-renewal, and differentiation in the intestinal epithelium. *Annu. Rev. Physiol.* **71**, 241-260.

van Es, J. H., van Gijn, M. E., Riccio, O., van den Born, M., Vooijs, M., Begthel, H., Cozijnsen, M., Robine, S., Winton, D. J., Radtke, F. et al. (2005). Notch/gamma-secretase inhibition turns proliferative cells in intestinal crypts and adenomas into goblet cells. *Nature* **435**, 959-963.

van Es, J. H., Sato, T., van de Wetering, M., Lyubimova, A., Yee Nee, A. N., Gregorieff, A., Sasaki, N., Zeinstra, L., van den Born, M., Korving, J. et al. (2012). Dll1 marks early secretory progenitors in gut crypts that can revert to stem cells upon tissue damage. *Nat. Cell Biol.* **14**, 1099-1104.

VanDussen, K. L., Carulli, A. J., Keeley, T. M., Patel, S. R., Puthoff, B. J., Magness, S. T., Tran, I. T., Maillard, I., Siebel, C., Kolterud, Å. et al. (2012). Notch signaling modulates proliferation and differentiation of intestinal crypt base columnar stem cells. *Development* **139**, 488-497.

Supplementary Table, Figures and Videos

Table S1. Oligonucleotides used for different approaches. (A) RT-qPCR study. (B) qPCR study after ChIP assay. (C) Probes used for EMSA.

S1A. Oligonucleotides used for the RT-qPCR study

cDNA detected (gene symbol)	Nucleotide sequence	Fragment length
Alkaline Phosphatase (intestinal-type)	F: CCAGCTTACCAATGAGAAGGA R: CTGGACCATTGCCATAGAGAA	146
Dll1	F: ATCTCCTTTCTCCTCTTTCC R: ACAACTTTCGGTTTCCTCTT	111
Dll4	F: CCCTCACCTGGATTACCTAC R: GAATCTGCTTGTTAGGGATG	147
emGFP	F: AGGACGACGGCAACTACAAG R: CTTGTGCCCCAGGATGTT	119
Glucagon	F: CGCTGATGGCTCCTTCTCTGAC R: CAAGTGACTGGCACGAGATGTTG	156
Hes1	F: CTACCCGTAAAGTCCCTAGCC R: AAAGCAACAAAATAACCACCAAA	103
Jag1	F: ACCAAGCTCAAGATCAAAAA R: TTTATTGCCAGGAACAACAC	141
Jag2	F: TGTCAGGCGGAAAACAAC R: GAGGACACACACACACACAC	122
Lysozyme	F: GCCAAGGTCTACAATCGTTGTGAGTTG R: CAGTCAGCCAGCTTGACACCACG	86
Muc2	F: AGAACGATGCCTACACCAAG R: CATTGAAGTCCCCGCAGAG	132
Notch1	F: TGTGGTGCCTCCTAGAGAAAA R: CTTTGGCAGTCAGGTGTTAGG	131
Notch2	F: GGGGGCAGGGTAGAGCAC R: GACGCAGATCGGGCATCTT	100
Ppib	F: CACCAATGGCTCACAGTTCTT R: ATGACATCCTTCAGTGGCTTG	156

S1B. Oligonucleotides used for qPCR study after ChIP assay

DNA detected (gene symbol)	Nucleotide sequence	Fragment length
Ctnnb1-TRE	F: ATGTGTGCTCAGGAAAACTGG R: CACTAGGTGATGGGCAGAGAC	236
Jag1-TRE1	F: CATGGCTCAGTTTTGATTGCT R: ATGCCTAGAAAACGCCCTACT	98
Jag1-TRE3	F: GGGTTCCCTTTGACCTTGATT R: CACAGAACTTGGCTTCTCCTG	115
Ppia	F: CCACTGTCGCTTTTCGCCGC R: TGCAAACAGCTCGAAGGAGACGC	109
Rplp0 (36B4)	F: TAAAAGATGTCCGCTCTCCTG R: TCCTTCAGCTCTTCTTTGCTC	110
Sfrp2-TRE	F: CTGGCACCTTACAATCCACTT R: TGGTCACCCATCCTGGTC	104
Villin	F: CAGACATACATGCAGGCAAAA R: CCAGATCCCTCTTCAGTGTGT	137

S1C. Probes used for EMSA

Gene	Nucleotide sequence
Ctnnb1-TRE	F: TGCTGAGGTGAGGTGAGGTGAGGCCAGGTCGTGGTC R: GACCACGACCTGGCCTCACCTCACCTCACCTCAGCA
Jag1-TRE1	F: TGCTGTGGGAGCTACTACTTTGACCTGACTTAATA R: TATTAAGTCAGGTCAAAGTAGTAGCTCCCACAGCA
Jag1-TRE2	F: ACATTGGCTTTGAACTTAGAGTGACCCTCCGGCCTCC R: GGAGGCCGGAGGGTCACTCTAAGTTCAAAGCCAATGT
Jag1-TRE3	F: GGGTTCCCTTTGACCTGATTTGACCAGGAGTGTCGC R: GCGACACTCCTGGTCAAATCAGGTCAAAGGGAACCC
Jag1-TRE3-Mut	F: GGGTTCCCTTTGGTCTGATTTGGTCAGGAGTGTCGC R: GCGACACTCCTGACCAAATCAGACCAAAGGGAACCC

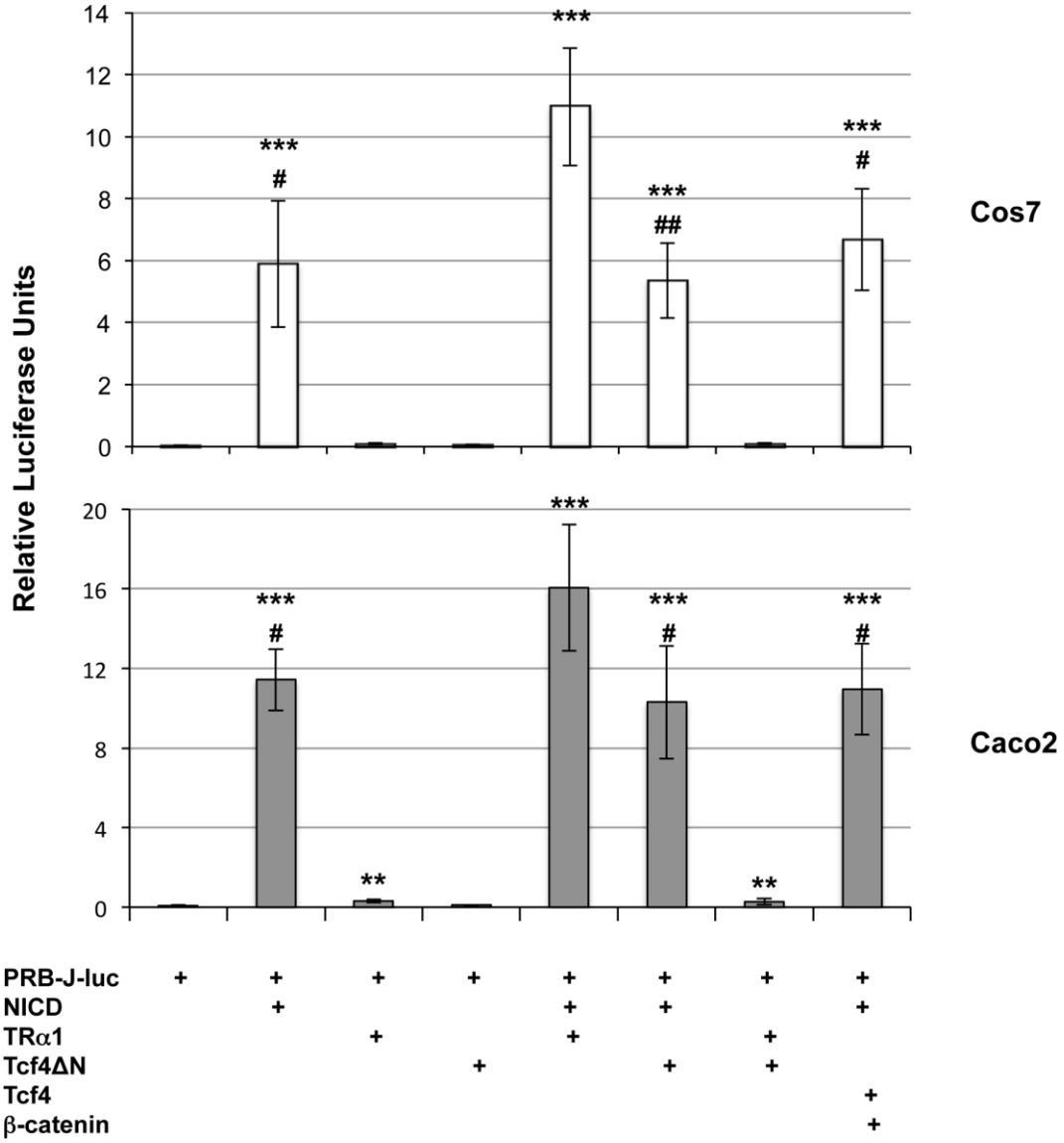

Figure S1. Notch activation by T3 and TRα1 *in vitro* is independent of the Wnt pathway.

The RBP-J luciferase reporter was transfected into Cos7 (upper panel) or Caco2 (lower panel) cells together with TRα1, NICD, a dominant-negative form of Tcf7l2 (Tcf4ΔN) or wild type Tcf7l2 (Tcf4) and β-catenin (the Wnt effectors) expression vectors as indicated. The cells were maintained in non-treated foetal serum containing physiological concentrations of T3. Pictures are representative of two independent experiments each conducted on six replicates; histograms depict the mean ± SD (n=6). *, P<0.05 and **, P<0.01 compared to the control condition (PRB-J-luc alone); #, P<0.05 and ##, P<0.01 compared to the NICD+TRα1 condition.

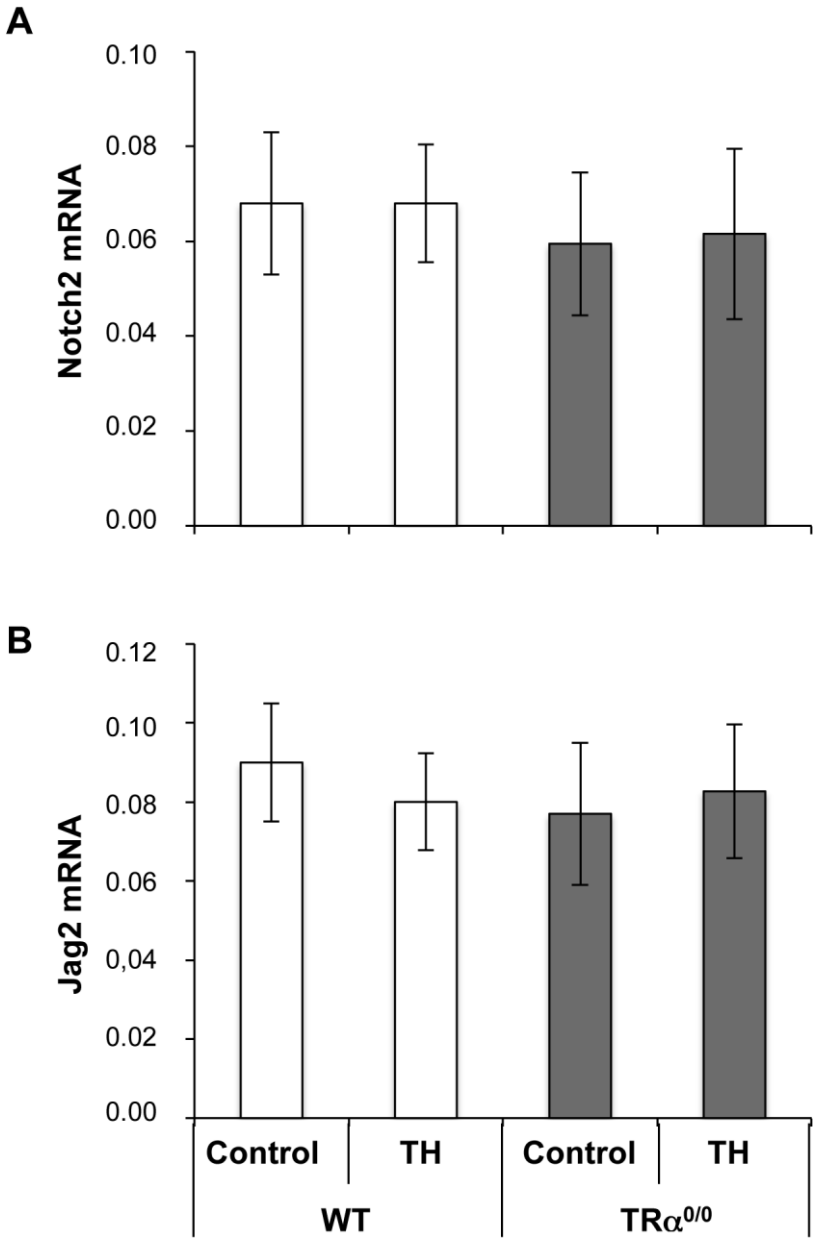

Figure S2. Analysis of Notch2 and Jag2 mRNA expression in WT and TRα$^{0/0}$ intestine. RT-qPCR experiments were performed to analyze the expression of Notch2 (A) and Jag2 (B), in WT (white bars) and TRα$^{0/0}$ (grey bars) animals treated or not with TH, as indicated. Histograms represent mean ± SD, N=3, after normalization with *Ppib*.

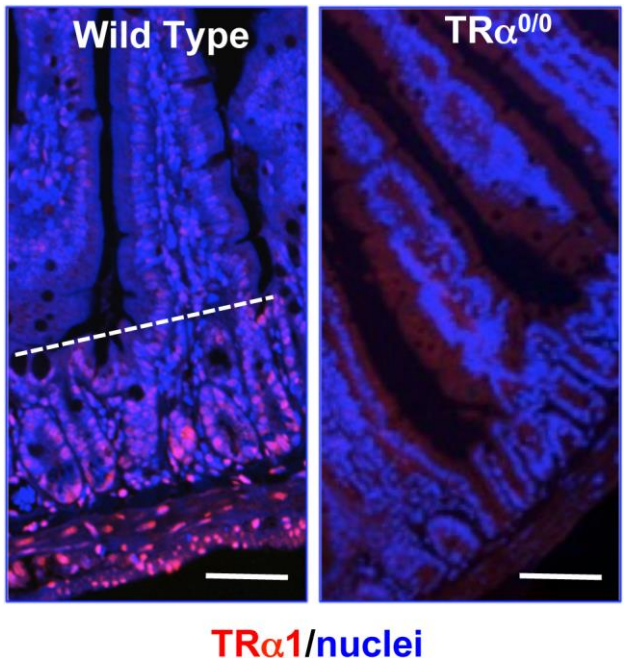

Figure S3. TRα1 is expressed in crypt epithelial cells. In the intestinal epithelium of wild-type animals, TRα1 is highly expressed in nuclei of crypt cells. However, it is worth highlighting that TRα1 is also expressed in nuclei of myofibroblasts and smooth muscle cells. As expected, TRα1 labeling is absent from intestinal sections of TRα$^{0/0}$ animals, confirming the specificity of the antibody used. The white dotted bar in the WT section shows the border between the crypts and the villi. Bars=30 μm.

Figure S4. Localization and *in vitro* analysis of the putative TRα1-binding sites on the *Jag1* promoter. A) A 5 kb region upstream of the *Jag1* start site was analyzed using NUBISCAN software, revealing three putative binding sites. The arrows indicate the location of the binding sites (TRE1, TRE2, TRE3), and the sequences underlined in bold show the arrangement of the half-sites as a typical DR4. The first exon is in red, and the first coding ATG is underlined. B) EMSA analysis using labeled TRE1, TRE2 and TRE3 probes and *in vitro*-transcribed/translated TRα1. Arrows indicate TRα1 binding at TRE1 and TRE3. The *Ctnnb1*-TRE probe was used as a positive control.

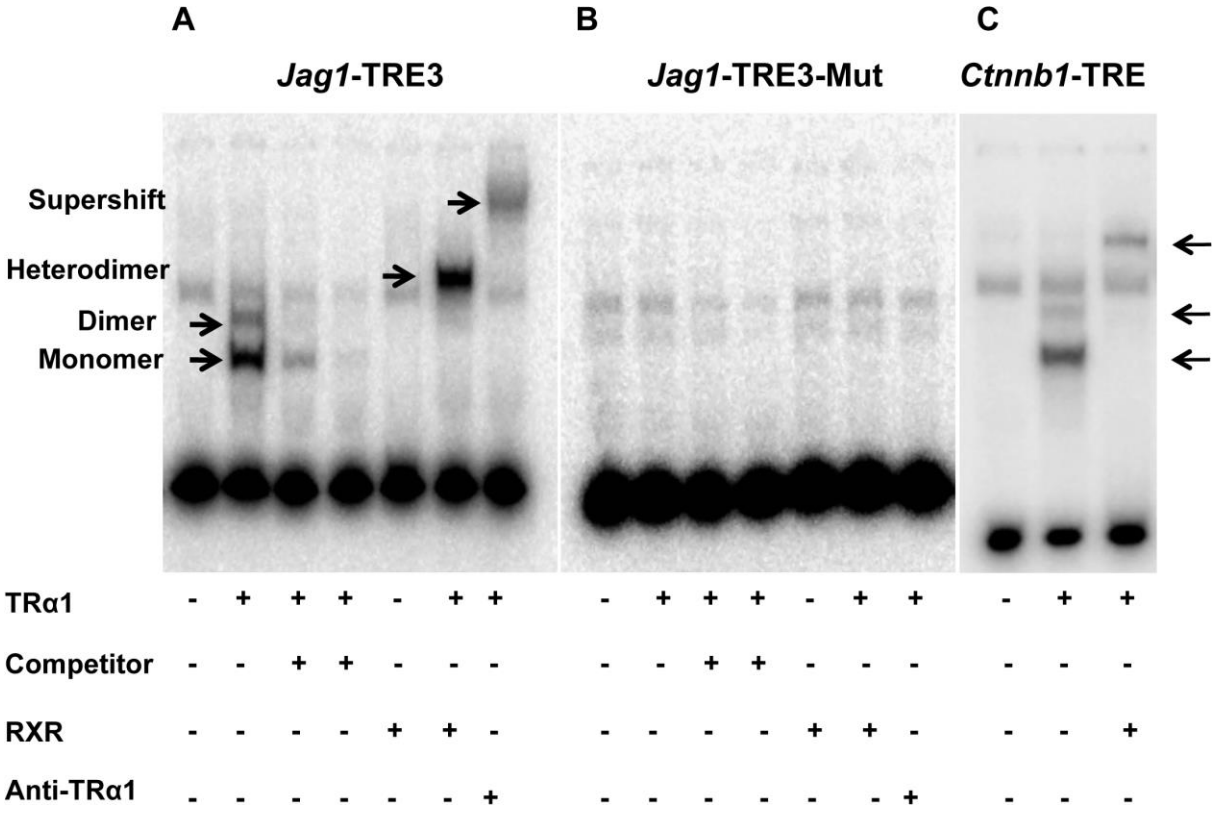

Figure S5. Electrophoretic mobility shift assay on the TRE3 present in the *Jag1* promoter. EMSA analysis using labeled Jag1-TRE3 (A) or Jag1-TRE-Mut (B) probes and in vitro-transcribed/translated proteins as indicated. Addition of specific cold sequences at increasing molar excess was used to assess the specificity of the binding. +, present; -, absent. Arrows indicate the TRα1 monomer and homodimer or the TRα1/RXR heterodimer binding the *Jag1*-TRE3. The addition of an anti-TRα1 antibody is able to induce a supershift of the TRα1-bound probe. The *Ctnnb1*-TRE (C) probe was used as a positive control.

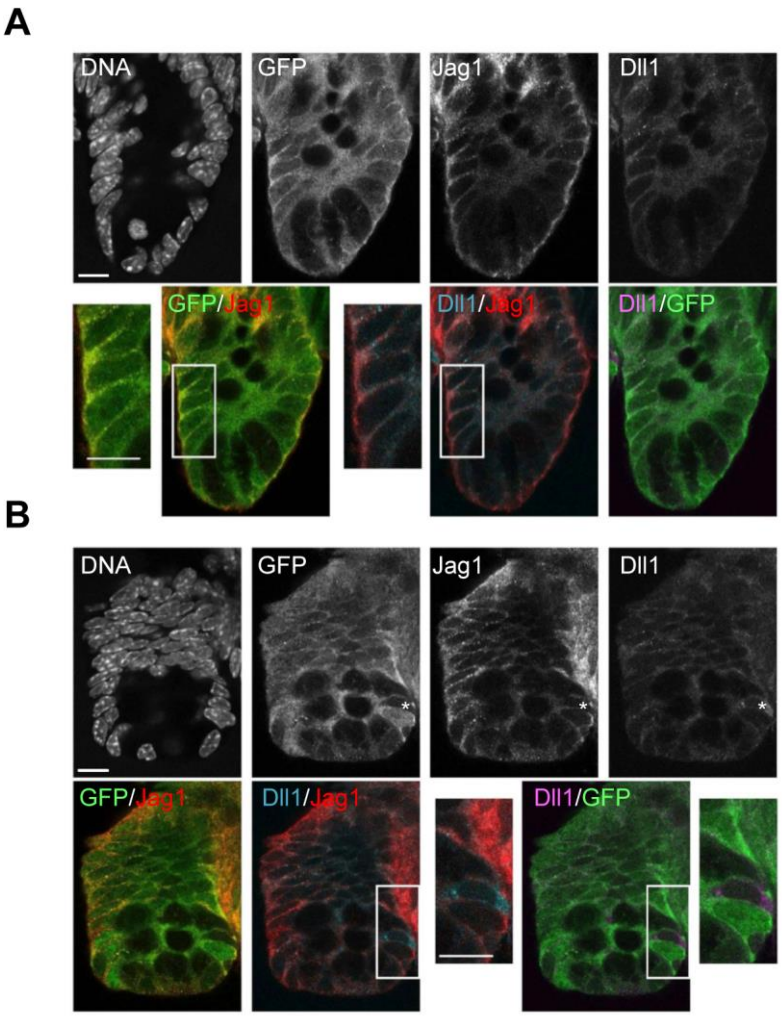

Figure S6. Pattern of Jag1 and Dll1 expression in the intestinal crypts. (A, B) *In toto* crypt immunostaining for Jag1 (red), GFP/Hes1 (green), Dll1 (cyan) and DNA, as indicated. All images represent maximum intensity projections of 3 consecutive focal planes (z= 0.48 μ m). White stars in the upper B panels indicate an exclusive Dll1-expressing cell. Bars = 10 μ m.

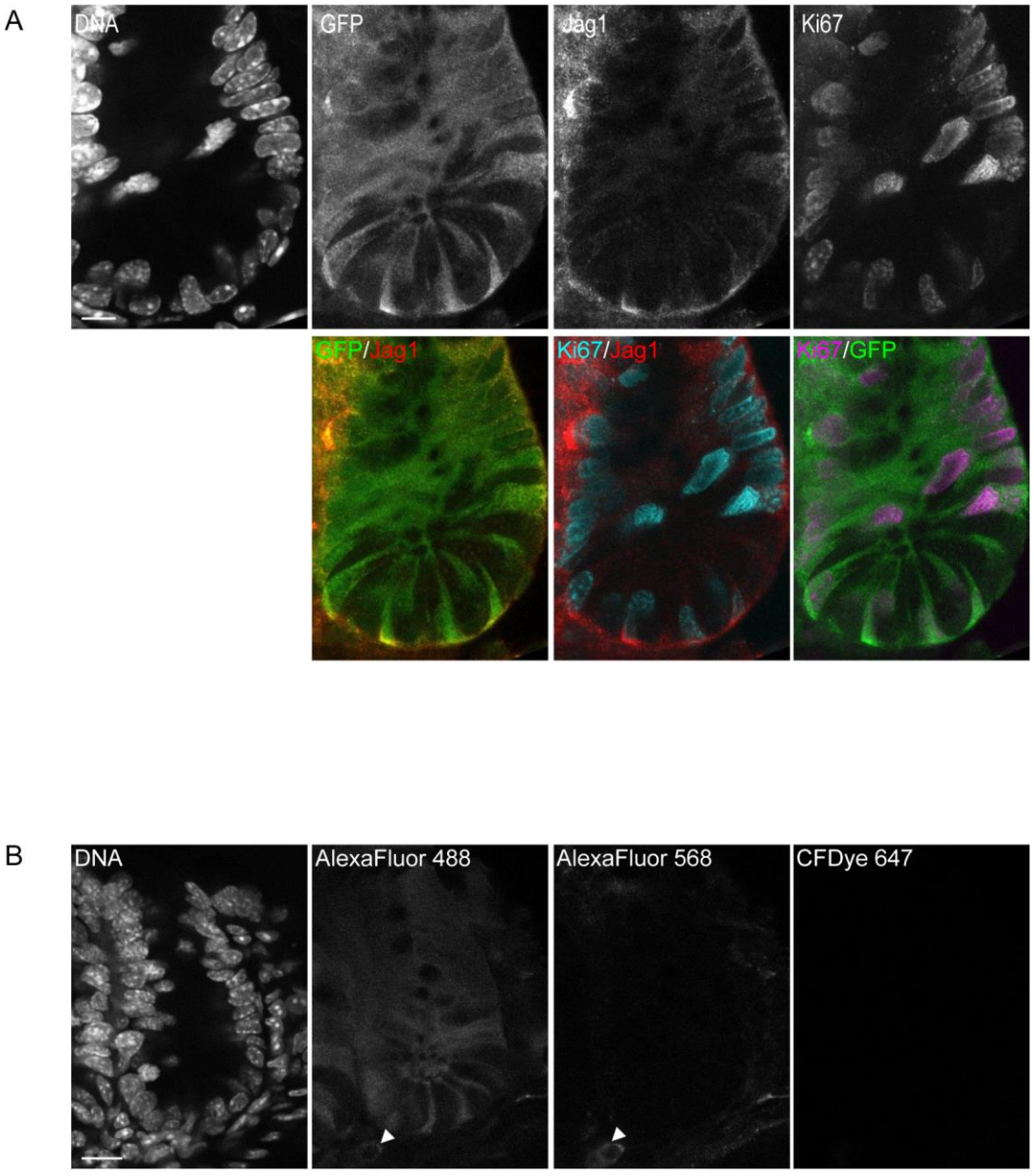

Figure S7. Complementary immunolabeling analysis in intestinal crypts. (A) Immunostaining for Jag1 (red), GFP/Hes1 (green), Ki67 (cyan) and DNA as indicated. (B) Images show negative control experiments to assess the specificity of the secondary fluorescent antibodies; these experiments were performed in the absence of primary antibodies. The native GFP/Hes1-positive cells are visualized with 488-nm laser illumination. White arrowheads indicate cells displaying non-specific labeling under 488-nm and 568-nm laser illumination. All images represent maximum intensity projections of 3 consecutive focal planes (z= 0.48 μm). Bars = 10 μm.

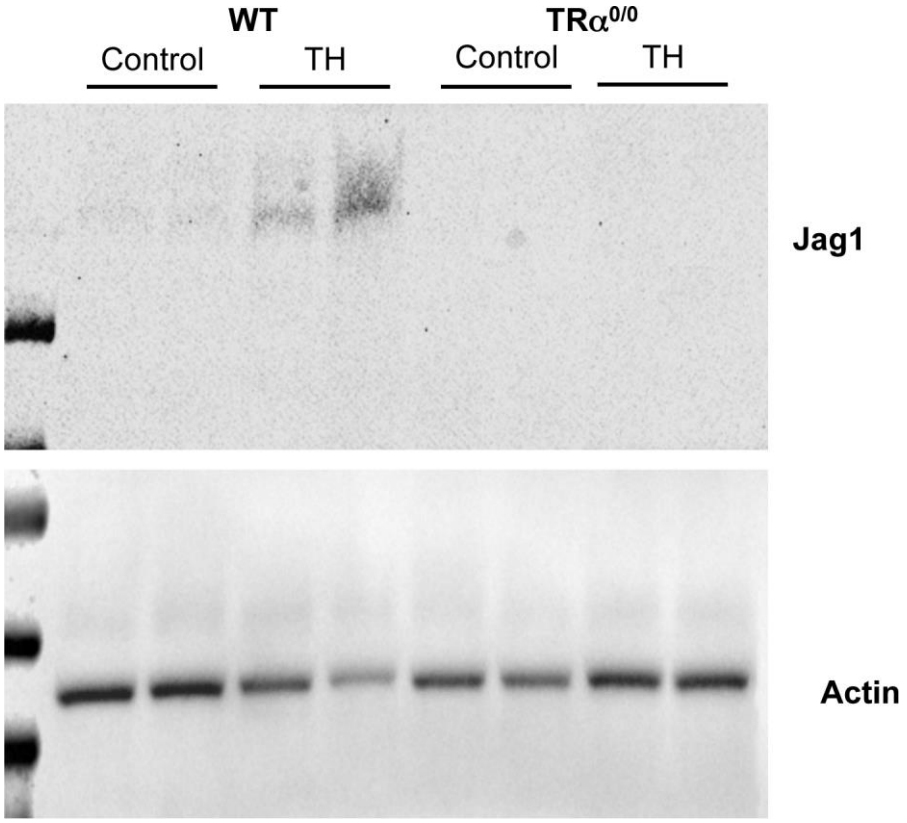

Figure S8. Study of Jag1 protein expression by western blot. WT and TRα$^{0/0}$ mice were treated or not with TH as indicated, and Jag1 expression was analysed in whole protein extracts from the intestinal mucosa. Actin was used as the loading control.

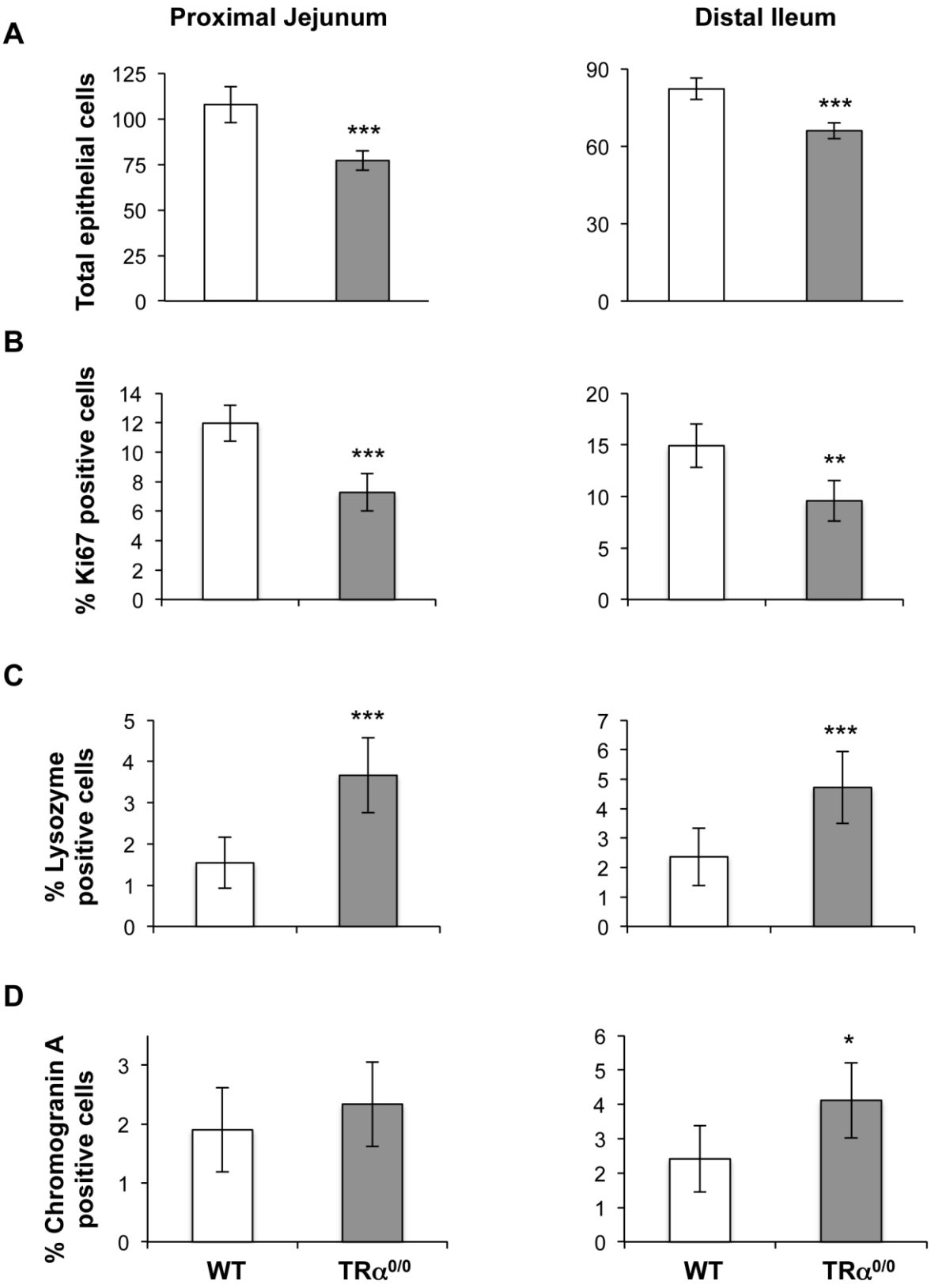
A
Proximal Jejunum
Distal Ileum
Total epithelial cells
125
100
75
50
25
0
***
90
60
30
0
***
B
% Ki67 positive cells
14
12
10
8
6
4
2
0
***
20
15
10
5
0
**
C
% Lysozyme positive cells
5
4
3
2
1
0
***
7
6
5
4
3
2
1
0
***
D
% Chromogranin A positive cells
3
2
1
0
WT
TRα0/0
6
5
4
3
2
1
0
*
WT
TRα0/0

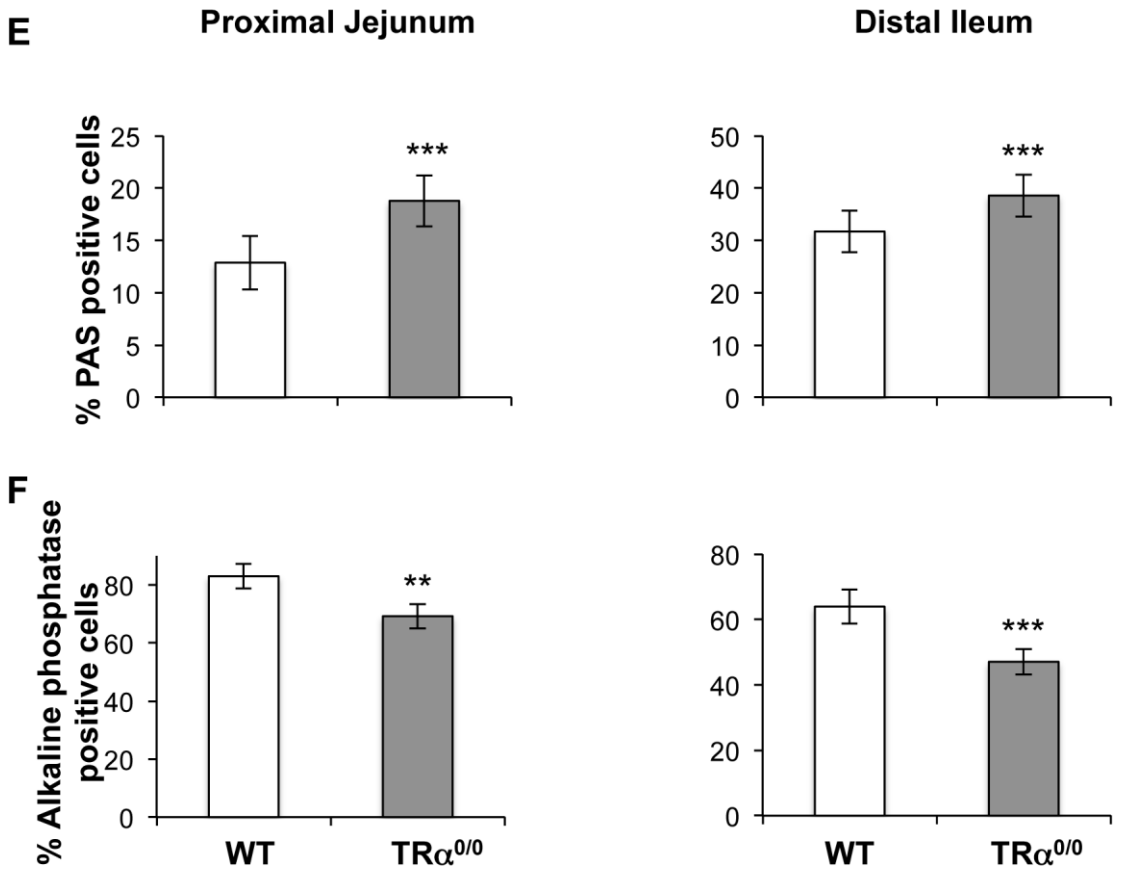

Figure S9. Analysis of intestinal epithelium features of the TRα$^{0/0}$ mice. Intestinal sections from WT (white bars) or TRα$^{0/0}$ (gray bars) mice were analyzed to evaluate alterations in epithelial cell number (A) or in the rates of cell proliferation (B) and cell differentiation (C-F) in both the proximal jejunum and the distal ileum as indicated. For the quantification of total cells and cells positive for each maker in the crypt-villus axes, approximately 30 axes were scored from at least four mice per genotype under the microscope. Histograms represent mean ± SD; N=30. *, P<0.05, **, P<0.01 and ***, P<0.001 compared to the WT.

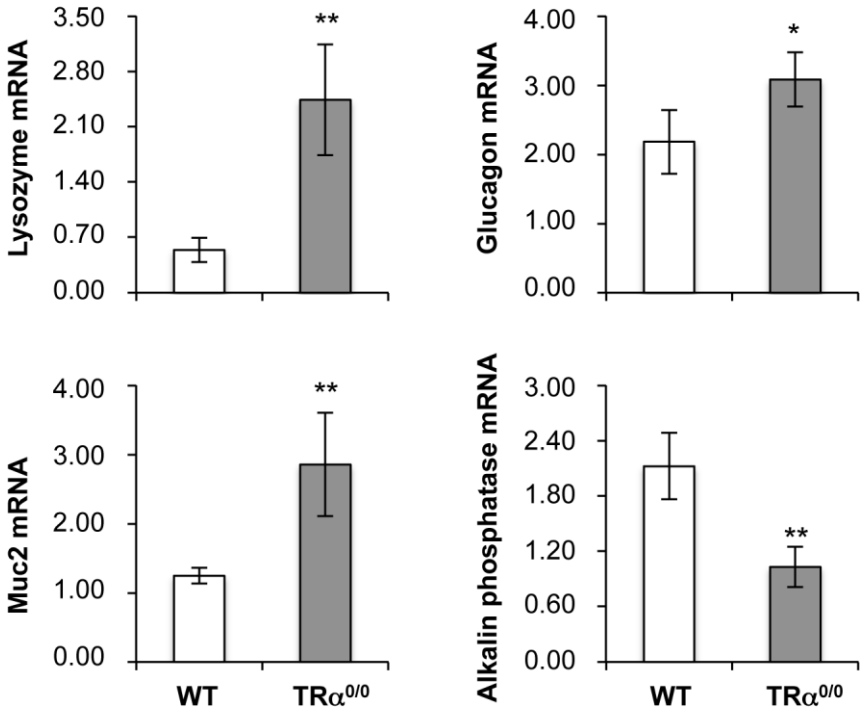

Figure S10. Analysis of differentiation marker's expression in WT and TRα$^{0/0}$ intestine. RT-qPCR experiments were performed to analyse the expression of lysozyme (Paneth cells), glucagon (enteroendocrine cells), Muc2 (goblet cells) and alkaline phosphatase (enterocytes), in the distal ileum of WT (white bars) and TRα$^{0/0}$ (grey bars) animals as indicated. Histograms represent mean ± SD, N=3, after normalization with *Ppib*. *, P<0.05 and **, P<0.01 compared to the WT.

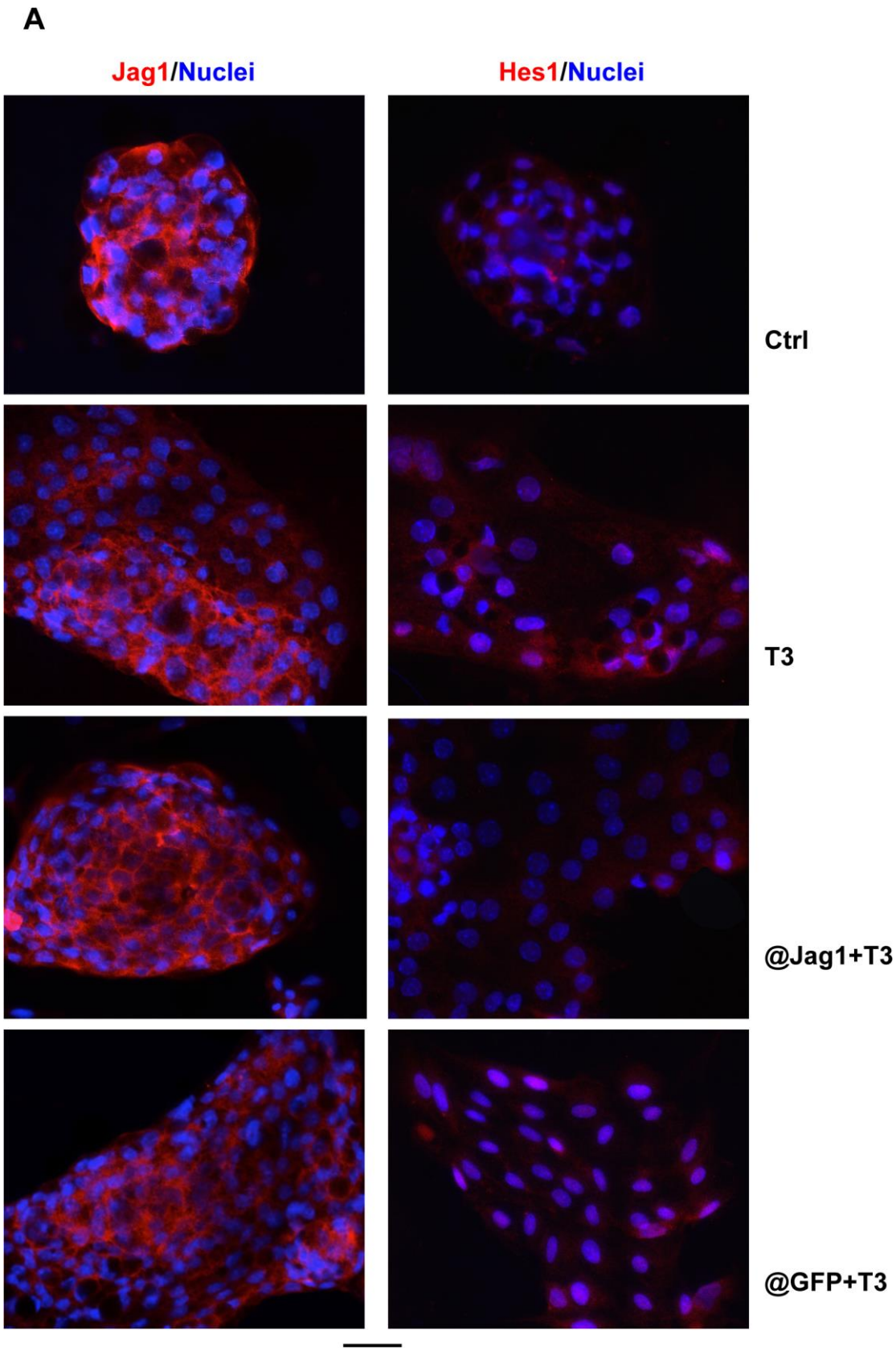
A
Jag1/Nuclei
Hes1/Nuclei
Ctrl
T3
@Jag1+T3
@GFP+T3

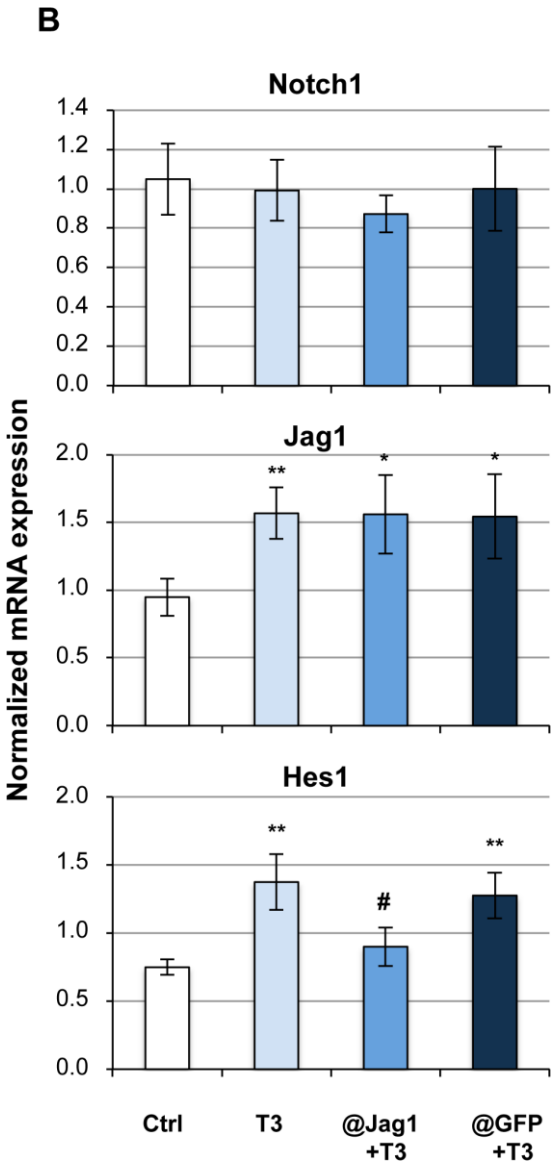

Figure S11. Supplementary data on functional link between T3-dependent Jag1 expression and Notch activity. A) Jag1 and Hes1 immunolabeling of intestinal epithelial primary cultures maintained in different conditions. The images show merged pictures of nuclear staining (blue) and specific staining (red) as indicated. They are representative of two independent experiments each conducted on triplicates. Bars, 20 μm. B) RT-qPCR analysis of the indicated mRNAs in cells maintained in different culture conditions. Graphs are representative of two independent experiments each conducted on duplicates; histograms depict the mean ± SD, N=4, after normalization with *Ppib*. *, P<0.05 and **, P<0.01 compared to the control condition; #, P<0.05 compared with T3 or @GFP+T3 conditions.

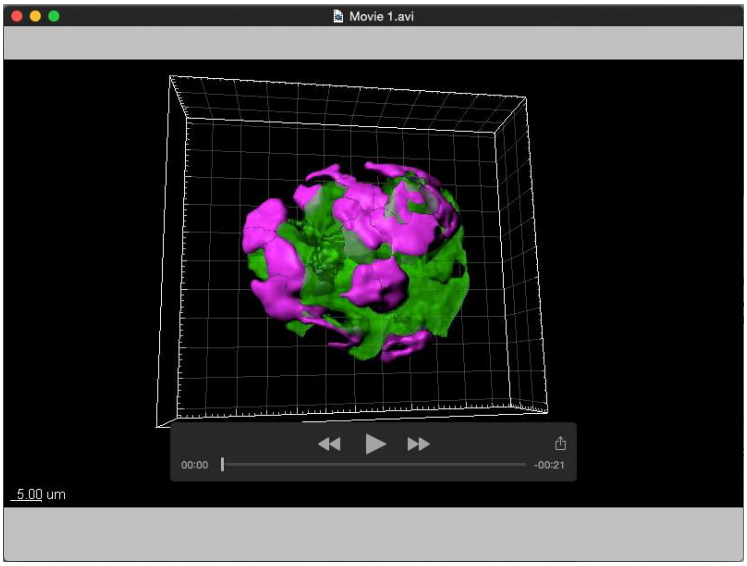

Movie 1. GFP/Hes1- and lysozyme-expressing cells in the crypts. 3D isosurface rendering of the fluorescent GFP/Hes1 (green) and lysozyme (magenta) signals observed in Figure 5C.

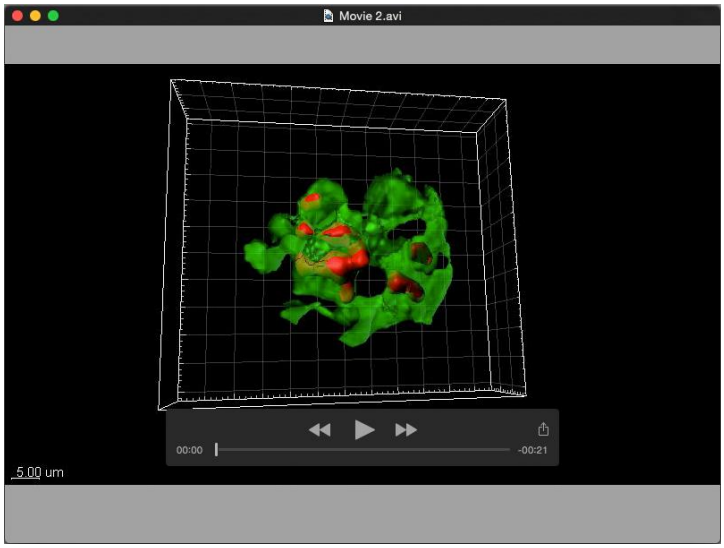

Movie 2. GFP/Hes1- and Jag1-expressing cells in the crypts. 3D isosurface rendering of the fluorescent GFP/Hes1 (green) and Jag1 (red) signals observed in Figure 5C. The green signal is 50% transparent to better visualize eventual signal overlap.

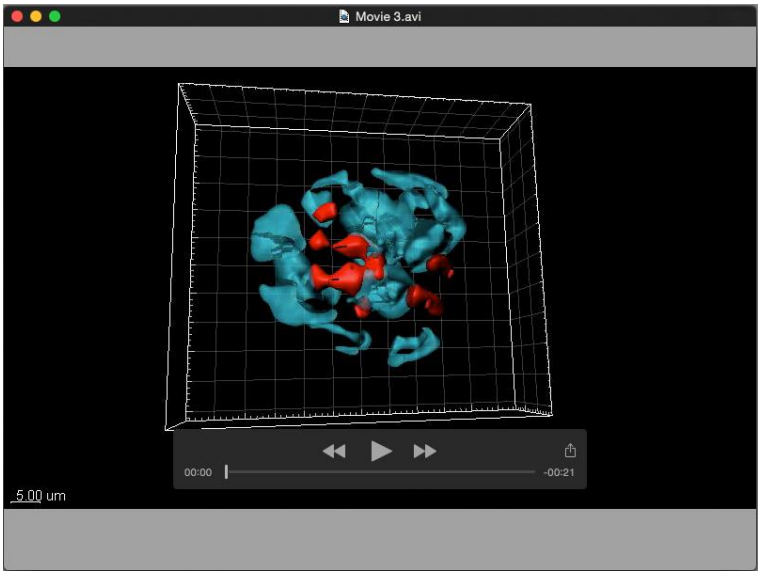

Movie 3. Jag1- and lysozyme-expressing cells in the crypts. 3D isosurface rendering of the fluorescent Jag1 (red) and lysozyme (cyan) signals observed in Figure 5C. The cyan signal is 50% transparent to better visualize eventual signal overlap.